



Nanoparticle–Polymer Synergies in Nanocomposite Hydrogels: From Design to Application

Tao Chen, Kai Hou, Qianyi Ren, Guoyin Chen, Peiling Wei, and Meifang Zhu*

Hydrogels are an important class of soft materials with high water retention that exhibit intelligent and elastic properties and have promising applications in the fields of biomaterials, soft machines, and artificial tissue. However, the low mechanical strength and limited functions of traditional chemically cross-linked hydrogels restrict their further applications. Natural materials that consist of stiff and soft components exhibit high mechanical strength and functionality. Among artificial soft materials, nanocomposite hydrogels are analogous to these natural materials because of the synergistic effects of nanoparticle (NP) polymers in hydrogels construction. In this article, the structural design and properties of nanocomposite hydrogels are summarized. Furthermore, along with the development of nanocomposite hydrogel-based devices, the shaping and potential applications of hydrogel devices in recent years are highlighted. The influence of the interactions between NPs and polymers on the dispersion as well as the structural stability of nanocomposite hydrogels is discussed, and the novel stimuli-responsive properties induced by the synergies between functional NPs and polymeric networks are reviewed. Finally, recent progress in the preparation and applications of nanocomposite hydrogels is highlighted. Interest in this field is growing, and the future and prospects of nanocomposite hydrogels are also reviewed.

1. Introduction

Hydrogels are soft materials with high water content and 3D cross-linked structures that consist primarily of homopolymers or copolymers. They have already been used in various fields including biomedicines,^[1–3] intelligent devices,^[4–6] and agriculture^[7,8] because of their specific properties, such as softness and elastic and intelligent properties. However, due to the heterogeneous distribution of cross-linking points in hydrogels, traditional chemically cross-linked hydrogels suffer from various drawbacks, such as low mechanical strength, a low degree of swelling, and a slow deswelling rate, which

have limited their widespread application.^[9–11] Therefore, the development of advanced hydrogel materials with desirable structures and enhanced mechanical performance has become essential and has inspired a large amount of research effort. For example, Gong et al.^[12] developed double network hydrogels (DN gels) formed by an interpenetrating polymer network (IPN) or semi-IPN, which exhibited outstanding mechanical properties with an elastic modulus of 0.1–1.0 MPa. Okumura et al.^[13] reported a series of topological hydrogels (TP gels), in which the figure-of-eight (such as α -cyclodextrin) polymers were introduced as cross-linkers to facilitate the free movement of polymer chains and thereby to dissipate the tension during severe deformations.

The nanocomposite hydrogel (NC gel) created by Haraguchi et al. is another important type of high-performance hydrogel. NC gels consist of immiscible stiff or soft components, and complex nanoscale structures.^[10,14,15] A wide range of nanoparticles (NPs), including ceramic

NPs (silica [SiO₂], titanium [TiO₂], etc.),^[16,17] metal or metal-oxide NPs (gold [Au], silver [Ag], iron oxide [Fe₃O₄], etc.),^[18–20] carbon-based nanomaterials (carbon nanotubes [CNTs] and graphene),^[21–23] and polymeric NPs (micelles, dendrimers, nanogels, etc.),^[24–26] were successfully introduced into NC gel networks by in situ polymerization, in situ growth of the NPs, or physical mixing (Figure 1).^[19,27,28] Comparing with neat polymeric hydrogels, the NPs play a significant role for the enhancement of the structural stability of NC gel due to the multiple interactions between NPs and polymers such as hydrogen bonds, van der Waals interactions, and electrostatic interactions. For example, the ionic bonds between cations of polymers and anions of NPs as strong cross-linkers, provide elasticity to NC gels. Moreover, the hydrogen bonds between amino or carboxyl of polymers and the oxygen-containing groups of the NPs as reversible cross-linking could dissipate destructive energy by breaking and reforming.^[29–31]

These NPs in the 3D polymer network not only serve as cross-linkers to reinforce hydrogels, but also endow the hydrogels with their characteristic functionalities. Furthermore, inspired by natural materials with well-ordered structures, NC gels with anisotropic and hierarchical fibrous structures have also attracted considerable attention recently. Because of their long-range ordered nanocomposite structure within the gel network matrix,

T. Chen, Dr. K. Hou, Q. Ren, G. Chen, P. Wei, Prof. M. Zhu
State Key Laboratory for Modification of Chemical Fibers
and Polymer Materials
College of Materials Science and Engineering
Donghua University
2999 North Renmin Road, Shanghai 201620, P.R. China
E-mail: zhurf@dhu.edu.cn

The ORCID identification number(s) for the author(s) of this article can be found under <https://doi.org/10.1002/marc.201800337>.

DOI: 10.1002/marc.201800337

hydrogels possess unique mechanical, optical, and biological properties that are comparable to those of natural soft tissues and enable adaptation to complex and dynamic environments.

In this article, based on the nanoparticle–polymer synergies, we aim to summarize the recent progress on NC gels from structural design to application (Figure 2). We give an overview of types of NPs introduced into NC gel, and then discuss the mechanical and stimuli-responsive properties associated with the NPs. Moreover, along with the development of NC gel-based devices, we summarize the novel-shaping strategies and NC gel devices with diverse morphologies in macroscope in recent years. Finally, we will highlight some of the recent representative research work with emphasis on the novel applications of NC gels in various fields, including soft actuators, sensors, drug delivery, and tissue engineering.

2. NPs for Nanocomposite Hydrogels

Different from neat polymeric hydrogels, the interaction between NPs and polymer is the structural foundation of NC hydrogels. NPs play a significant role for enhancement of the structure of NC gel due to the multiple interactions between NPs and polymers including hydrogen bonds, van der Waals interactions, and electrostatic interactions. Three main strategies have been widely used to introduce NPs into NC hydrogels including in situ polymerization, in situ growth of the NPs, and physical mixing.^[19,27,28] In situ polymerization is suitable for NPs with polar group on surface such as carboxyl (-COOH), hydroxyl (-OH), and amino (-NH₂), for example, laponite, graphene oxide, dendrimers, which can form strong hydrogen bonds and electrostatic interactions with monomers.^[19,31,32] And then the in situ polymerizations of hydrogels were occurred to obtain hydrogels with stable structure and excellent mechanical properties. In situ growth of NC gels is usually suitable for NPs with intrinsic functions but hardly surface modified, for example, polyaniline NPs, metal and metal-oxide NPs.^[27,33] Physical mixing is a simple route to compound NC gels by polymer and NPs directly. This strategy is not suitable to prepare hydrogel with excellent mechanical properties due to the weak interactions between polymers and NPs.^[28] However, this strategy is appropriate for 3D printing, because the compounding of polymers and NPs is an effective method to enhance the viscoelasticity of polymer solution for extrusion in 3D printing, that will be discussed in Section 4.

In this section, on the basis of the progress of NC gels recently, we emphasize on the classification of common and new types of NPs, and mainly focus on the dispersion and interactions of NPs in hydrogel. In addition, the functional and constructional influences of NPs are also reviewed.

2.1. Carbon-Based NPs

Carbon-based nanomaterials, such as CNTs and graphene, have been considered as ideal components to substantially improve the performance of NC gels due to their excellent multifunctionality, unique physicochemical and dimensional properties.^[22,34] However, the fabrication of homogeneous,



Tao Chen received his M.S. from Stevens Institute of Technology in 2014, majoring in material science and engineering. Currently, he is a Ph.D. candidate under the supervision of Prof. Meifang Zhu at Donghua University. He is working on the construction and application of novel hydrogel fiber materials.



Kai Hou received his Ph.D. from Donghua University in 2018. He currently holds a postdoctoral position at the college of Material Science and Engineering, Donghua University. He is working on the establishment of dynamic cross-linking spinning for the large-scale production of hydrogel fiber from monomer solution. This novel spinning technology

holds broad promise for fiber formation from traditionally non-spinnable monomers.



Meifang Zhu is a professor at Donghua University in the College of Material Science and Engineering, State Key Laboratory for Modification of Chemical Fibres and Polymer Materials. She obtained her bachelor's and master's degrees in chemical fibers at the Textile University of China (now named Donghua University) in 1986 and 1988, respectively.

In September 1999, she received her Ph.D. degree from Donghua University jointly with the University of Dresden in Germany. She then began teaching at Donghua University. Her research interests include organic–inorganic hybrid materials, nanocomposite hydrogel materials, biomass fiber, and biomedical materials.

coherent, and transparent gels with pristine carbon nanomaterials is difficult because of the hydrophobic intrinsic property of carbon materials. Therefore, the poor interfacial compatibility between carbon materials and polymeric networks makes it difficult to form a strong coupling between the two components for a desirable architecture.^[35] Therefore, hydrophilic groups, such as -COOH, -OH, and pyridine

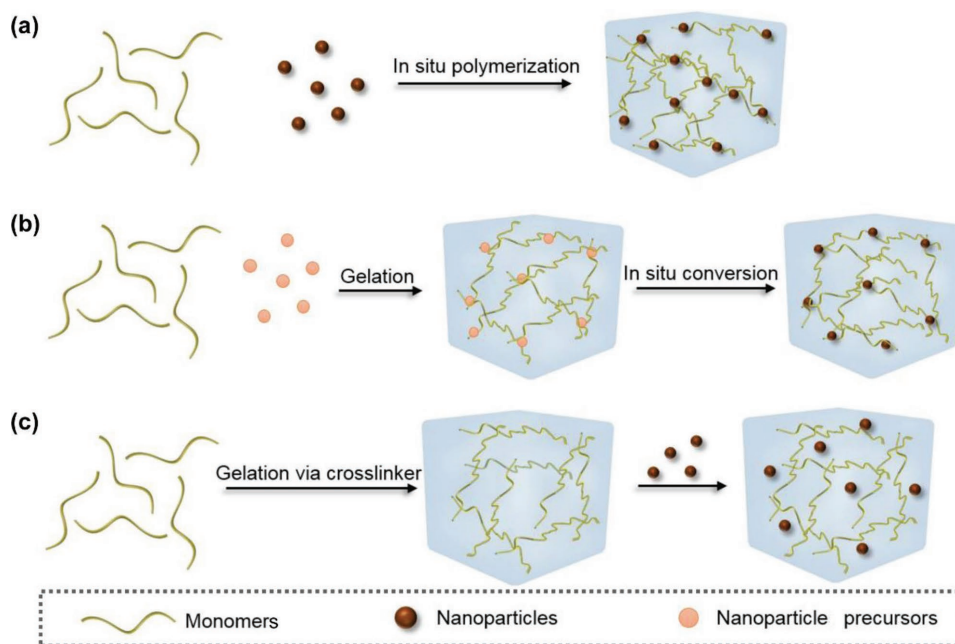


Figure 1. Approaches used to fabricate NC gel. a) In situ polymerization of monomer in nanoparticle suspension; b) reactive nanoparticle synthesis within gelled materials; c) physical embedding of nanoparticles into the hydrogel matrix after gelation.

groups, are normally introduced on the surface of CNTs or graphene through surface modification of the carbon materials to increase the interfacial bonding between carbon and the polymer matrix.^[35–37] For example, pyridine-functionalized CNTs were prepared by pyridine diazonium salt treatment and introduced into the poly(acrylic acid) (PAA) to prepare a

polyelectrolyte CNTs/PAA NC gel.^[38] The hydrogen bonding between pyridine groups grafted with CNTs and the carboxylic groups of the PAA is believed to play a significant role in strengthening the hydrogel networks.

Because the chemical functionalization disrupts the electronic structure of pristine carbon nanomaterials, which reduces

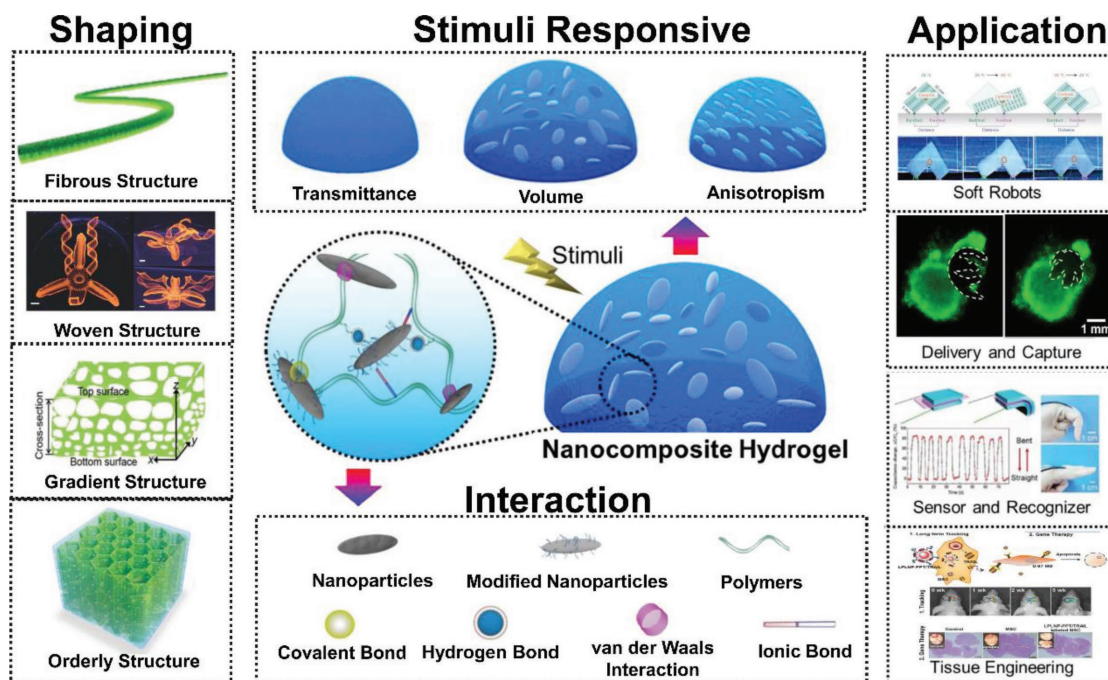


Figure 2. Schematic illustration of the structural design of nanocomposite hydrogels from polymer–nanoparticle interaction (covalent bonds, van der Waals interactions, ionic bonds, hydrogen bonds) to external stimuli, and their potential application fields in soft robots, sensors and recognizers, delivery and capture, and tissue engineering.

the conductivity of composite gels,^[38] physical approaches, such as polymer wrapping^[39,40] and cellulose-assisted dispersion,^[41,42] have been developed. Polymer wrapping, a common technique that facilitates the transfer of carbon nanomaterials to the aqueous phase, involves the utilization of polymers containing aromatic groups, such as polystyrenesulfonate, which can wrap around carbon materials through π - π stacking and hydrophobic-hydrophilic interactions. For example, NC gels consisting of poly(*N*-isopropylacrylamide) (PNIPAAm) and PAA-micelle-encapsulated CNTs were prepared by Bai et al.^[40] These encapsulated CNTs with cross-linked polymer shells were obtained via a photo-cross-linking reaction of the self-assembly of amphiphilic azide diblock copolymers around CNTs. The polymer shell was demonstrated to improve the CNTs dispersibility and the interactions between encapsulated CNTs (E-CNT-PAA) and PNIPAAm (Figure 3a). However, the polymer wrapping method might induce a relatively weak adhesion between the wrapping molecules and the carbon nanomaterials.

In addition, this surface coverage with polymer can perturb the carbon-carbon contacts necessary for electron transfer.

The cellulose-assisted method enables the dispersal of carbon nanomaterials in aqueous media to form long-term stable colloidal dispersions. Hamedi et al. found that the dispersive action of nanocellulose is caused by fluctuations in the counterions on the surface of the nanocellulose, which is helpful for forming attractive interactions between the carbon nanomaterials and nanocellulose.^[42] Taking advantage of this behavior, Fu et al. fabricated a poly(acrylamide) (PAAm) NC gel using cellulose nanofiber (CNF) as a CNT dispersion agent, and the as-prepared hydrogel exhibited excellent mechanical properties (Figure 3b) and electrical performance due to the ideal dispersion of CNTs.^[41]

In summary, the addition of carbon-based NPs endows NC gels with improved mechanical and multifunctional properties.^[43] However, the complicated processing approaches, the low transparency, and the concern about *in vivo* biocompatibility of the carbon-based NC gels are still on a rapid development path.

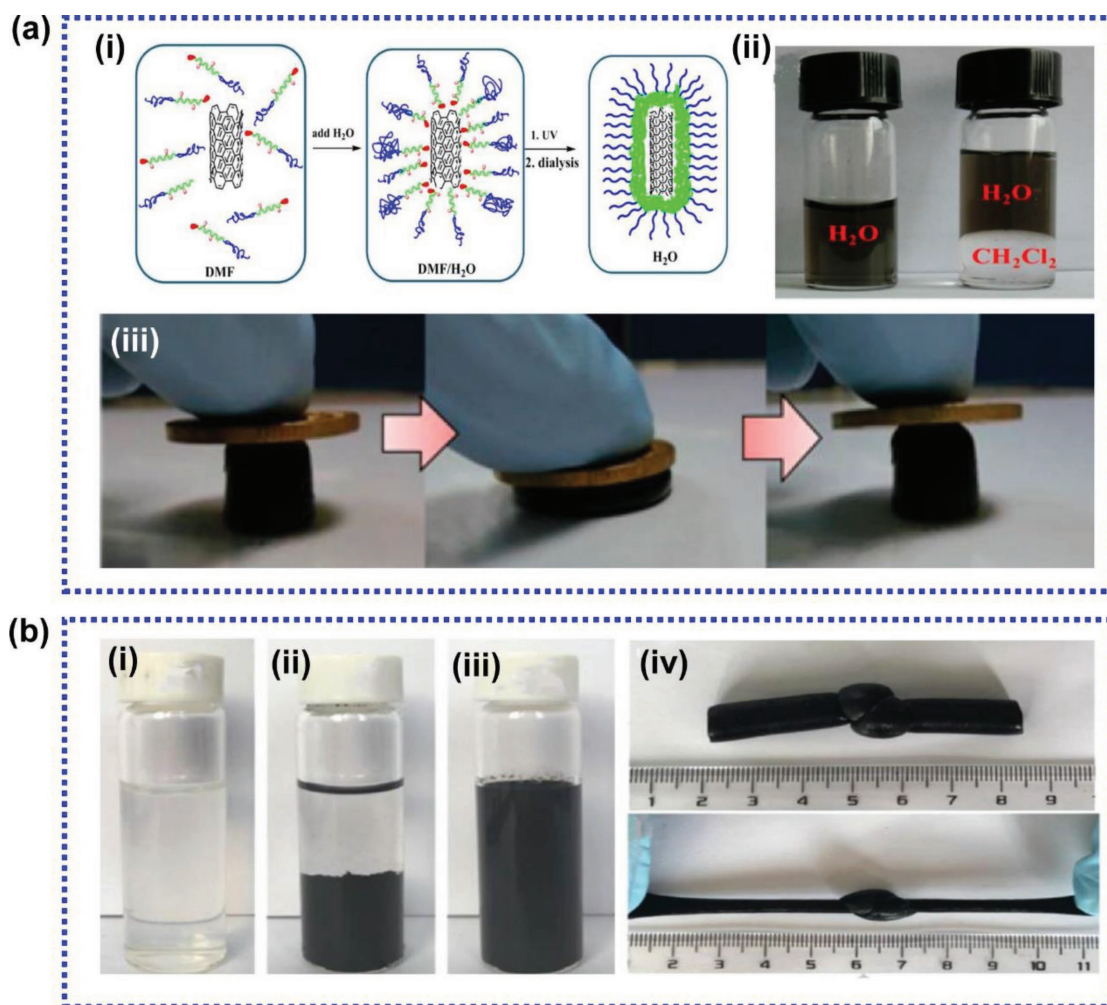


Figure 3. Methods of CNT dispersion and corresponding NC gels. a) CNT dispersion with encapsulation copolymers: i) schematic illustration of the encapsulation of a CNT with amphiphilic block copolymers and cross-linking under UV irradiation (254 nm); ii) photographs of the dispersion of E-CNT-PAA in H₂O and a mixed solvent of H₂O and CH₂Cl₂; iii) photographs of PNIPAAm/(E-CNT-PAA) composite hydrogel under pressure and recovery. Reproduced with permission.^[40] Copyright 2017, American Chemical Society. b) CNT dispersion with incorporated CNF: i) photographs of the CNF dispersion; ii) CNT dispersion without CNF, and iii) CNT/CNF (wt% = 10:3) dispersion; iv) photographs of PAAm/(CNT-CNF) NC gel showing excellent mechanical properties: knotting and stretching with a knot. Reproduced with permission.^[41] Copyright 2018, American Chemical Society.

2.2. Metal and Metal-Oxide NPs

With the increasing popularity of hydrogels in various biomedical and biomimetic applications such as bioimaging, biosensing, and biotracking, there is a growing need to engineer hydrogels with magnetic, electrical, and optical stimulative properties. Metal and metal-oxide NPs possess these unique properties that cannot be obtained from polymers. Due to the intrinsic antibacterial,^[44] ferromagnetic,^[45] and conducting properties,^[46] metal and metal-oxide NPs can provide NC gels with antimicrobial activity, magnetic and electrical properties which are suitable for biomedical applications. Therefore, metal and metal-oxide NPs are ideal reinforcing materials with great potential in preparing NC gels with unique characteristics and tunable properties.^[46] Diverse metallic NPs, including Au, Ag, noble metal, and metal-oxide NPs, such as titanium oxide (TiO₂), iron oxide (Fe₃O₄), and zirconia (ZrO₂), have been successfully used to manufacture NC gels.^[19,21,47,48]

However, due to the high surface energy and strong dipole-dipole attractions among metallic NPs, achieving a stable dispersion in aqueous solution remains a challenge. Two main methods have been developed to synthesize metallic NC gels with a good dispersion of metallic NPs. The first is the in situ growth of metallic NPs in the hydrogel matrix after gelation.^[49] Typically, hydrogels with a 3D network structure not only act as a container for loading metallic NPs but also serve as a reactor for the nucleation and growth of NPs. The second is the use of reactive metallic NPs as cross-linkers to produce hydrogels with free-radical polymerization.^[27,50–52] Compared with the first embedding method, the latter approach results in metallic NC gels with mechanical strength enhanced by strong interfacial interactions between the polymer and surface-modified metallic NPs. Specifically, a PNIPAAm/Au NC gel was prepared by the free-radical polymerization of *N*-isopropylacrylamide (NIPAM) monomer in an aqueous medium containing Au⁺ ions.^[53] During the cross-linking polymerization process, catechol groups were introduced into the PNIPAAm networks. The catechol groups act as reducing agents for Au⁺ ions to enable the functionalization of the PNIPAAm network with Au NPs and the simultaneous reinforcement of the hydrogel structure.

2.3. Inorganic Clay NPs

Clays, a series of minerals with diverse dimensions, such as SiO₂ (0D), halloysite-nanotubes (1D), montmorillonite (2D),

and synthetic hectorite (2D), are extensively used as nanofillers in NC gels.^[32,54] One frequently used material is clay nanoplatelets, such as montmorillonite (MMT) and synthetic hectorite (laponite). The structure of laponite clay nanoplatelets is illustrated in **Figure 4**. Each layer of the clay nanoplatelets consists of one octahedral sheet sandwiched by two tetrahedral sheets. The octahedral sheets usually contain cations, such as aluminum (Al) ions and magnesium (Mg) ions, which are octahedrally coordinated by oxygen, while the tetrahedral sheets consist of silicon dioxide with negative charges due to partial isomorphous substitution, typically of Al³⁺ by Mg²⁺ in montmorillonite and of Mg²⁺ by Li⁺ in laponite.^[54] The basal plane of these clay minerals has a permanent negative charge due to the isomorphous substitution of cations within the octahedral and/or tetrahedral layers by cations with lower valence. Because hydroxyl groups occur on the edges of clay minerals, the charge of the clay edge depends on the pH of the suspension medium. The acidity of these hydroxyl groups is dependent on the type of cations within the tetrahedral and octahedral sheet. In general, the edge charge is positive in acidic suspension media and negative in basic suspension media.^[32] Distinct from other NPs, exfoliated 2D nanoclays (approximately 100 × 100 × 1 nm³ for montmorillonite)^[55] with negative charge in polymeric networks endow the resulting hydrogels with remarkable mechanical properties because of their interfacial interactions. Haraguchi et al. succeeded in preparing a series of NC gels with good flexibility and transparent properties that can be treated as rubbery materials. Notably, the content of clay can be varied to tailor the mechanical properties and the swelling/deswelling kinetics of NC gels.^[15] Specifically, PNIPAAm/laponite NC gels with extraordinary high tensile strength (1.1 MPa) and modulus (453 KPa) have been reported because the flexible polymer chains between the clay sheets could be elongated extensively and reversibly without breaking.^[10] On the other hand, due to the high biocompatibility of inorganic clay NPs, the NC gels containing these NPs possess good potential applications as biomaterials.

The optimal exfoliation of clay is a critical issue for its role as a nanofiller in NC gels. For instance, MMT and laponite consist of several paralleled layers, which are usually packed one above another with exchangeable hydrated cations located between the layers.^[55] In order to prepare NC gels with high mechanical performance, the electrostatic forces between the negatively charged clay nanoplatelets and the interlayer cations must be overcome. Because the swelling of the layered structure depends on the exchangeable cations or intercalated species

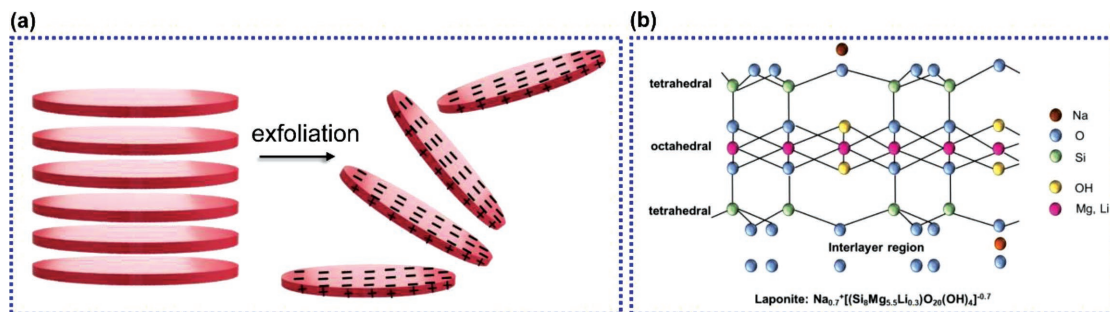


Figure 4. Schematic drawing of a) laponite tactoids and the exfoliation of laponite and b) the structure of laponite.

in the interlayer space, the introduction of easily hydrated cations (e.g., Na⁺) and organic cations is considered to be an effective approach to the exfoliation process.^[56] The exfoliated inorganic clay nanoplates can then be successfully introduced into polymer networks to form NC gels. For example, sodium pyrophosphate can form chelate complexes at the clay edge with cations of the octahedral sheet, resulting in edges with a permanent negative charge.^[57] Having the same charge on the surfaces and edges leads to strong electrostatic repulsion between clay nanoplatelets and thus efficiently prevents their agglomeration. Laponite XLS is a type of clay modified by this method that can be dispersed easily in water to form a homogeneous solution with low viscosity even at a relatively high clay concentration (under 10 wt%). In our previous work, we fabricated PNIPAAm/Laponite XLS NC gels with extremely high tensile strength (≈1 MPa), which was attributed to the uniform dispersion of clay nanoplatelets with high density in the hybrid hydrogels.^[58]

2.4. Polymeric NPs

A series of polymeric NPs, such as dendrimers,^[26] hyperbranched polymers,^[59] micelles,^[24] nanogels,^[60] and core-shell NPs,^[61] have also been developed for use in NC gel systems for various applications. Because polymeric NPs usually possess multiple functional groups, NC gels can be endowed with multifunctionality by the incorporation of these NPs into the hydrogel network via covalent or non-covalent interactions. Polymeric NPs-embedded hydrogels have attracted great attention for biomedical applications, including drug delivery and tissue engineering, due to their ability to entrap hydrophilic or hydrophobic drugs with enhanced mechanical properties.^[62]

Dendrimers and hyperbranched polymeric NPs are attractive because of their highly branched and spherical structure, which presents abundant surface functional groups, resulting in better loading efficiency and higher reactivity than those of hydrogels made from linear polymers.^[26,63] For example, poly-amidoamine dendritic NPs were physically incorporated within collagen scaffolds to improve their mechanical stiffness, structural integration, and promotion of human conjunctival fibroblast proliferation, which are attributed to the numerous interactions within the hydrogel network.^[64] In another example, the limitations of poor drug loading efficiency and lack of control over dendritic NPs with lower degrees of branching were both overcome by incorporating hyperbranched poly(amino ester) (HPAE)-5 NPs into hydrogel networks.^[65] The periphery of the hyperbranched polymeric NPs was modified with photo-cross-linkable moieties to form a covalently cross-linked network via UV exposure. The resulting hydrogel allowed the controlled release of active ingredients for more than a week, which was otherwise difficult to achieve with conventional hydrogels prepared from linear polymers.

In addition to biomedical applications, polymeric NPs could also be used to impart mechanical strength to hydrogels. For example, a PAAm and polystyrene (PS) NP composite hydrogel with excellent mechanical properties was prepared by a facile method in our group.^[66,67] This composite hydrogel was fabricated using in situ free-radical polymerization with PS NPs

as cross-linkers. Due to the uniform dispersion of NPs and multicategory interactions among polymer chains, this composite hydrogel displays excellent mechanical properties and physicochemical stability. In addition, PS NPs were developed by embedding Fe₃O₄ NPs through miniemulsion polymerization.^[48] These hybrid PS NPs acted as both cross-linkers and photoinitiators in PAAm hydrogel polymerization. The resulting hydrogel displayed both good mechanical properties and high magnetic sensitivity, suggesting potential applications in magnetic devices and microfluidic valves.

3. Properties of Nanocomposite Hydrogels

NC gels not only could be prepared by several kinds of NPs or polymers, but also could be obtained either by chemically cross-linking polymers, or by physically cross-linking polymers.^[2,21] The way in which NC gels are made can affect many properties of NC gels, such as mechanical, optical, and stimuli-responsive properties. In this section, some outstanding properties of NC gels are discussed from synthesis approaches to further applications.

3.1. Mechanical Properties

Appropriate mechanical properties are indispensable for hydrogel applications. However, traditional chemically cross-linked hydrogels, such as *N,N'*-methylenebisacrylamide (BIS) cross-linked hydrogels, have the disadvantage of weak mechanical properties due to the heterogeneous distribution of their polymer chains and molecular weights among cross-linking points.^[66] Specifically, in heterogeneous chemically cross-linked hydrogels, increasing the overall stress applied to the polymer chains induces chain fracture and finally results in the destruction of the hydrogel structure.^[58] In the past 10 years, many novel strategies have been adopted to enhance the mechanical properties of hydrogels via rational molecular and structural design.^[68–72] Among the resulting materials, NC gels have proven to be promising for improving the mechanical properties of hydrogels effectively due to their excellent NP–polymer synergies.

Typically, due to the reversible physical interactions between polymers and NPs, the overload mechanical stress on the NC gels could be effectively dissipated by spreading along with the polymer chains mutually rather than concentrated. As a result, the NC gel is less likely to form micro cracks under mechanical stress, which avoids widespread failure and endows the NC gel with good mechanical properties.^[33,58]

To effectively enhance the mechanical properties of NC gels, improving the dispersion of NPs is essential. For example, a PNIPAAm/clay NC gel that exhibited remarkable increases in tensile strength and modulus was prepared by Haraguchi.^[10] This hydrogel could be elongated by more than 1000% due to the excellent exfoliation and dispersion of clay in the hydrogel. The nanoscale exfoliation and dispersion of clay nanoplatelets into hydrogels helped to narrow the length distribution of the polymer chains and avoid the concentration of stress, finally resulting in superior tensile properties of the NC gel.

The multiple non-covalent interactions between NPs and polymers are the main reason that NP dispersion improves the mechanical properties of NC gels. In contrast with the covalently cross-linked hydrogels, the amount of non-covalent interactions, such as hydrogen bonds, van der Waals interactions, and electrostatic interactions among NPs and polymers play significant roles in the enhancement of mechanical properties due to the reversibility of cross-links and the flexibility of polymer chains. For example, a PAAm/graphene oxide (GO) NC gel was fabricated by the in situ polymerization of acrylamide (AAM) with dispersed GO as a cross-linker.^[29] The PAAm/GO NC gel containing only 0.0079 wt% GO exhibited a tensile strength of 385 KPa and break elongation of 3435%. This improvement is attributed to the effective stress dissipation because of the non-covalent cross-links in the structure, such as hydrogen bonds between the amide groups of PAAm and the carboxylic groups of GO. Recently, cationic poly(acrylamide-*co*-2-(dimethylamino)ethylacrylamethochloride) (P(AAm-*co*-DAC)) hydrogels containing GO as cross-linkers were fabricated by Liu et al.^[30] This NC gel displayed good mechanical properties due to the multiple non-covalent interactions between P(AAm-*co*-DAC) and GO (including ionic interactions between $N(CH_3)^+$ of DAC and COO^- of GO, and hydrogen bonds between NH_2 of AAm and the oxygen-containing group of the GO), which provided elastic and reversible cross-linking to dissipate energy out. As shown in **Figure 5**, this P(AAm-*co*-DAC)/GO NC gel exhibited not only good mechanical properties, but also excellent self-healing efficiency because of the multiple interactions between polymer and GO.

In addition to the non-covalent interactions between NPs and polymers, physical entanglement among polymer chains could also enhance mechanical properties. For example, poly(NIPAAm-*co*-AAM)/clay NC gels exhibit a higher tensile modulus due to the synergistic effects of side chains with different lengths and the main chains.^[14] In particular, PAAm molecular chains possess favorable elasticity due to hydrophilic $-CONH_2$ side chains, while PNIPAAm molecular chains are more rigid than those of PAAm because of the hydrophobic containing $-CONH(CH_3)_2$ side chains. When a tensile stress was applied to P(NIPAAm-*co*-AAM)/clay NC gels, the main chains of PNIPAAm were stretched, extended, and rearranged, whereas the side chains of PAAm with their flexible hydrophilic groups influenced the interactions between the poly(NIPAAm-*co*-AAM) chains and clay. This dynamic chain entanglement was significant for improvements in the mechanical strength of hydrogel.

Recently, the combination of multiple interfacial interactions between polymers and NPs (such as non-covalent bonds and physical entanglement) has also been found to enhance the mechanical properties of hydrogel remarkably. For example, micelle-encapsulated CNTs were incorporated with PNIPAAm as cross-linkers to obtain a mechanically tough PNIPAAm/(E-CNT-PAA) NC gel.^[40] The encapsulated CNTs were obtained by the self-assembly of amphipathic azide deblock copolymers. The tensile strength and elongation of the NC gel were at least 3.5 times higher than those of neat PNIPAAm hydrogels. This enhancement of the mechanical properties was attributed to three aspects of the synergistic effects of CNTs and polymers: i) the good dispersion of encapsulated CNTs; ii) the hydrogen

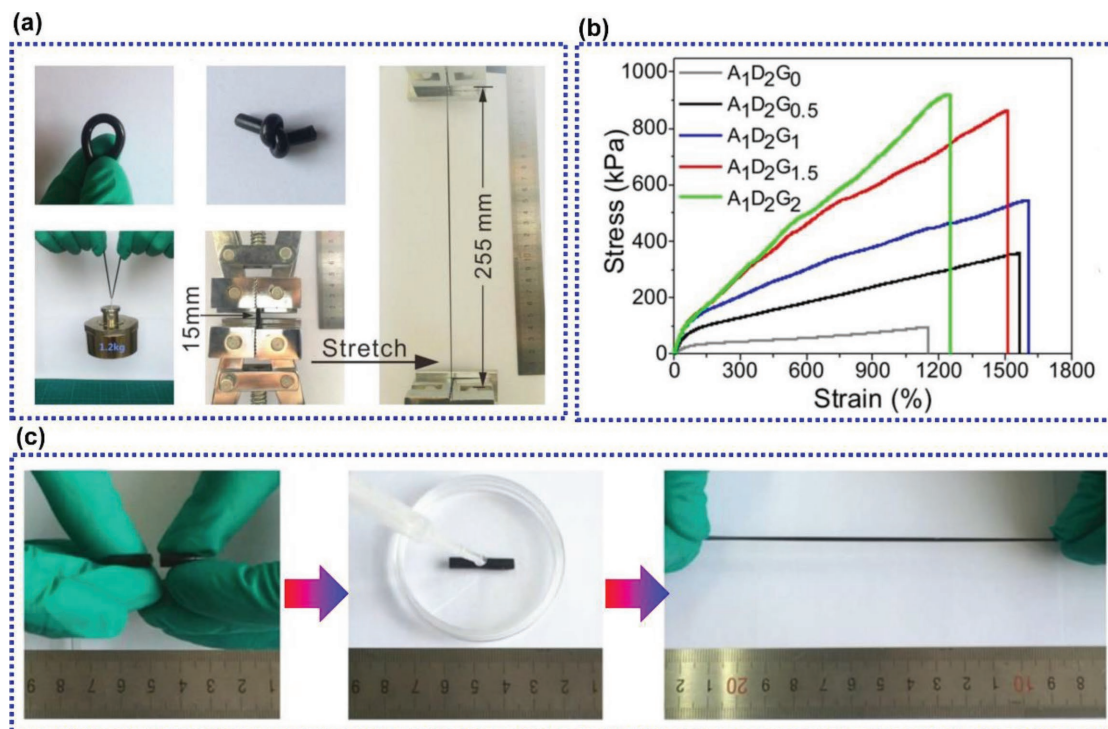


Figure 5. Mechanical properties and self-healing properties of P(AAm-*co*-DAC)/GO composite hydrogels. a) The NC gels can be bent, knotted, loaded, and stretched. b) The tensile stress–strain curves of the NC gels with different GO contents. c) A cylinder of the NC gel sample was cut in half; the two-halves were contacted and a droplet of water was dropped on the cut surface for self-healing; after standing for hours, the healed sample can be stretched to a large strain. Reproduced with permission.^[30] Copyright 2017, American Chemical Society.

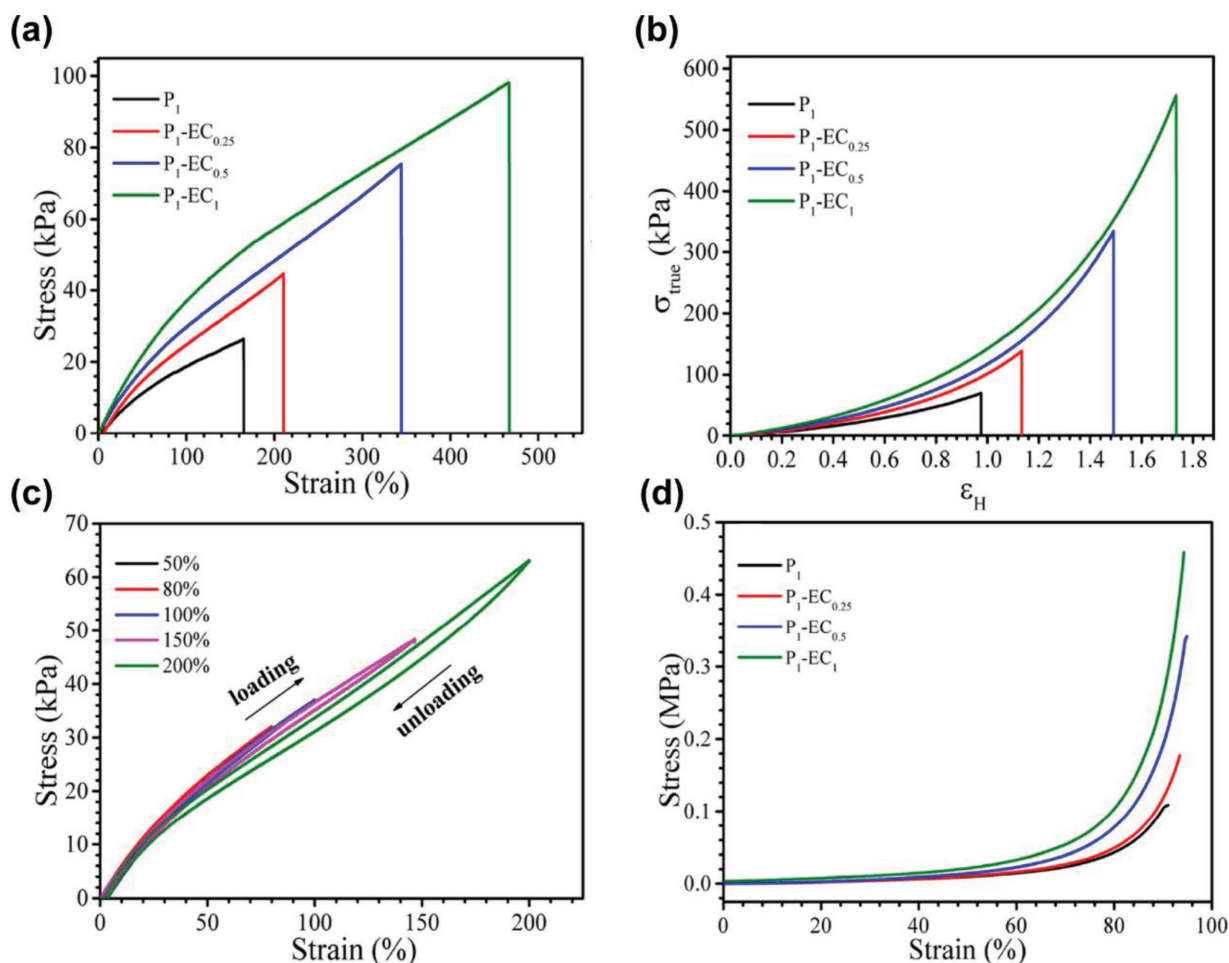


Figure 6. Mechanical properties of the PNIPAAm/E-CNT-PAA composite hydrogels. a) Tensile stress–strain curves of the NC gel. b) True stress–true strain curves of the NC gel. c) Tensile stress–strain curves of the NC gel during loading–unloading cycles. d) Typical compressive stress–strain. Reproduced with permission.^[40] Copyright 2017, American Chemical Society.

bonds between carboxylic groups of the micelle and the amide groups of PNIPAAm; and iii) the entanglements between the polymer chains of the micelle and PNIPAAm. A scheme illustrating the encapsulated CNTs and the mechanical properties of the NC gel is shown in **Figure 6**.

In addition, a new type of NC gel with gradient structure that exhibits anisotropic mechanical properties has recently been produced. When external fields are applied during the gelation process, such as direct current (DC) electric fields,^[73–75] magnetic fields,^[76,77] and stress,^[78] NPs tend to form an orderly dispersion in the NC gels, revealing anisotropic mechanical properties due to the anisotropic microstructure of the hydrogels. We will discuss the NC gel with anisotropic structure in Sections 3.2.4, 3.2.5, and 4. Here, we have selected and summarized some NC gels with enhanced mechanical properties, as shown in **Table 1**.

3.2. Stimuli-Responsive Properties

The stimuli-responsive hydrogels can undergo reversible physical or chemical changes after being exposed to external

stimuli, such as pH, temperature, light, electric and magnetic fields.^[89,90] By combination of diverse NPs and polymers, the NC gels could obtain or strengthen multiple stimuli-responsive properties. In this section, we will summarize the influence of functional NPs on the enhancement of the stimuli-responsive properties of NC gels.

3.2.1. pH-Responsive NC Gels

Polymeric hydrogels with ionic pendant groups can respond to the environmental pH because of their abilities to accept and donate protons. The resulting change in the net charge of the ionized pendant group results in a rapid volume change in a pH-sensitive NC gel due to the electrostatic repulsion among the ionized groups. There are two types of common pH-responsive hydrogels: cationic (such as PAAm with amine groups) and anionic (such as PAA with carboxylic groups) hydrogels. Due to the synergies of NPs and polymers, NC pH-responsive hydrogels possess specific properties that differ from those of traditional pH-responsive hydrogels and have promising potential for use.^[91,92]

Table 1. Comparison of the tensile mechanical properties of various nanocomposite hydrogels.

Nanocomposite hydrogels	Tensile strength [kPa]	Elongation at break [%]	Elastic modulus [kPa]	Ref.
PVA-CNT	2060.1	267	570.0	[79]
PAAm/CNT-PAA	82.3	508	420.2	[39]
PNIPAAm/CNT-PAA	97.4	465	–	[40]
PAAm/GO	385.2	3435	28.5	[29]
PAA/BIS/GO	27.1	300	–	[80]
PAAm/SDBS/GO	155.4	2869	36.6	[81]
PAA/Fe ³⁺ /GO	776.8	2980	50.7	[82]
PAAm/GPO	650.2	3500	52.3	[83]
PNIPAAm/Laponite	68.8	1112	4.0	[10]
PNIPAAm/Laponite XLS	1000.0	1348	74.18	[58]
PAAm/Laponite XLS	271.0	2509	10.8	[14]
P(NIPAAm-co-AAm)/Laponite XLS	58	2004	–	[84]
P(DMA-co-GMA)/Laponite XLG	13.7	>900	–	[85]
P(NIPAAm-co-DAC)/Laponite RDS	250	450	–	[86]
P(AMPS-co-AAm)/MMT	90.1	1618	–	[87]
P(MEO ₂ MA-co-OEGMA)/Laponite XLS	63.6	1145	29.37	[88]

GO nanosheets show amphiphilic characteristics due to the existence of hydrophilic groups, such as –OH and –COOH, on the hydrophobic graphene nanosheets. Meanwhile, the dispersion of GO nanosheets in aqueous medium depends on the environmental pH. In a strong acidic medium, GO nanosheets tend to aggregate because of insufficient mutual repulsion due to the protonation of the –COOH groups.^[93] Therefore, GO containing a pH-responsive NC gel always exhibits a gelation state under acidic conditions and a gel–sol transition in alkaline medium. For example, PAA/GO NC gels containing a great number of –COOH groups belonging to both the polymer and the GO deswelled at low pH (<4.5) and swelled dramatically at higher pH (>4.5) due to the ionized –COOH groups (pK_a of PAA = 4.3).^[94] The swelling ratio of the PAA/GO NC gel was affected by both pH and GO fraction.

In addition, the dispersion of nanoclays such as montmorillonite and laponite is pH-dependent due to their edge charges, which influence the ionization of the polymer in response to pH. For example, a pH/temperature dual-responsive NC gel was prepared by the incorporation of laponite into poly(diethylacrylamide (DEA)-co-(2-dimethylamino) ethyl methacrylate) (DMAEMA).^[95] The swelling ratio of the hydrogels varied in buffer of different pH values. DMAEMA is a pH-sensitive monomer due to the protonation of its tertiary amino groups, which results in the most obvious swelling ratio at lower pH (such as pH = 2). The protonation of the tertiary amine group promotes water uptake into the hydrogel and therefore swelling due to the enhanced electrostatic repulsive forces among positively charged ammonium groups. As a result, the swelling ratio of poly(DEA-co-DMAEMA)/clay NC gel in an acid environment was greater than that in an alkaline environment, making these hydrogels promising for potential applications in the biomedical field.

3.2.2. Temperature-Responsive NC Gels

Since the pioneer Tanaka discovered the temperature-responsive property of PNIPAAm hydrogel, thermo-responsive hydrogels have attracted considerable attention due to their potential applications in many fields, including drug release, optical device, and separation-adhesion.^[11,49,96] Generally, two types of thermo-responsive hydrogels have been defined. One type shows a phase transition from water-insoluble to soluble at the upper critical solution temperature (UCST).^[4] There are many UCST-type polymers, including natural polymers such as gelatin and synthetic polymers such as PAA.^[90] In contrast, other polymers show lower critical solution temperature (LCST) behavior, which means that the hydrogels undergo a phase transition from soluble to insoluble when the temperature is above the LCST. Most LCST-type polymers contain hydrophilic groups, such as (–CONH–), and hydrophobic parts (–R–).^[4] The synthetic polymer PNIPAAm, a well-known example of the LCST-type polymers, has been intensively investigated in recent decades.

In thermo-responsive NC gels, the thermally induced volume change can be varied depending on the synergies of NPs with polymers, making the swelling ratio of thermo-responsive NC gels dependent on the NP fractions. With increasing NP content (higher cross-linking density), the polymer chains between the cross-linking points became relatively short and too rigid to display a substantial volume change. For example, PNIPAAm/GO/clay hydrogels were prepared by in situ polymerization.^[97] This NC gel underwent a rapid volume shrinkage at 34 °C because of the LCST of PNIPAAm at ≈32 °C. GO nanosheets and clay nanoplatelets in the hydrogels both restrained the volume expansion during the swelling process. As a result, hydrogels with higher GO fractions exhibited a lower swelling ratio. Moreover, the response temperature of thermo-responsive

NC gels can be adjusted by controlling the polymer–NP interactions. Specifically, the conformational shift of the PNIPAAm chain from hydrophilic coil to hydrophobic globular formation upon heating above LCST ($\approx 32\text{ }^{\circ}\text{C}$) is significantly confined by clay. The main reason is that with the increasing content of clay, which forms hydrophilic edges and hydrophobic surfaces, the hydrophilic–hydrophobic balance of PNIPAAm hydrogel becomes influenced by the clay fractions, and as a result, the LCST of PNIPAAm/clay NC gels is higher than that of normal PNIPAAm hydrogel.^[32]

To overcome the monotonous phase transition temperature (approximately $32\text{ }^{\circ}\text{C}$) in traditional PNIPAAm-based hydrogels, our group recently prepared a novel NC gel with precisely tunable UCST and LCST.^[4] The thermo-responsive NC gel was free-radically copolymerized in situ by 2-(2-methoxyethoxy) ethyl methacrylate (MEO₂MA) and oligoethyleneglycol methacrylate (OEGMA) with inorganic clay (Laponite XLS) as a physical cross-linker. This novel P(OEGMA-*co*-MEO₂MA)/clay NC gel not only exhibited UCST and LCST simultaneously, but also allowed the precise tuning of UCST and LCST over a wide temperature range (between 5 and $85\text{ }^{\circ}\text{C}$) by adjusting the content of OEGMA monomer and clay. As shown in **Figure 7a,b,c**, the UCST and LCST were linearly influenced by OEGMA content owing to the change in hydrophilic properties influenced by the side chains of OEGMA. In addition, the UCST and LCST were

nonlinearly influenced by clay content. Notably, lower clay content hardly induced the phase transition of hydrogel polymer chains, and higher clay content restricted the flexibility of the P(OEGMA-*co*-MEO₂MA) chains. These novel thermo-responsive NC gels could be applied in smart devices to monitor environmental temperature changes by detecting the irradiance intensity of a laser, as illustrated in **Figure 7d**.

3.2.3. Light-Responsive NC Gels

Light is an attractive stimulus due to its remote controllability, high accuracy, and adjustable transmission and intensity, and therefore, light-responsive materials are uniquely advantageous for various applications. For example, some nanomaterials, such as carbon-based and semiconductor NPs, possess photothermal conversion properties, that is, the ability to absorb near infrared (NIR) light ($700\text{--}1100\text{ nm}$) and transform it into heat because of their favorable photothermal conversion properties and high thermal conductivity. Thus, the combination of photothermal NPs with thermo-responsive polymers could endow traditional thermo-responsive hydrogels with light-responsive properties. For example, a novel PNIPAAm/GO NC gel could be used as a remote light-controlled liquid microvalve.^[98] In this device, GO could absorb NIR irradiation and then convert

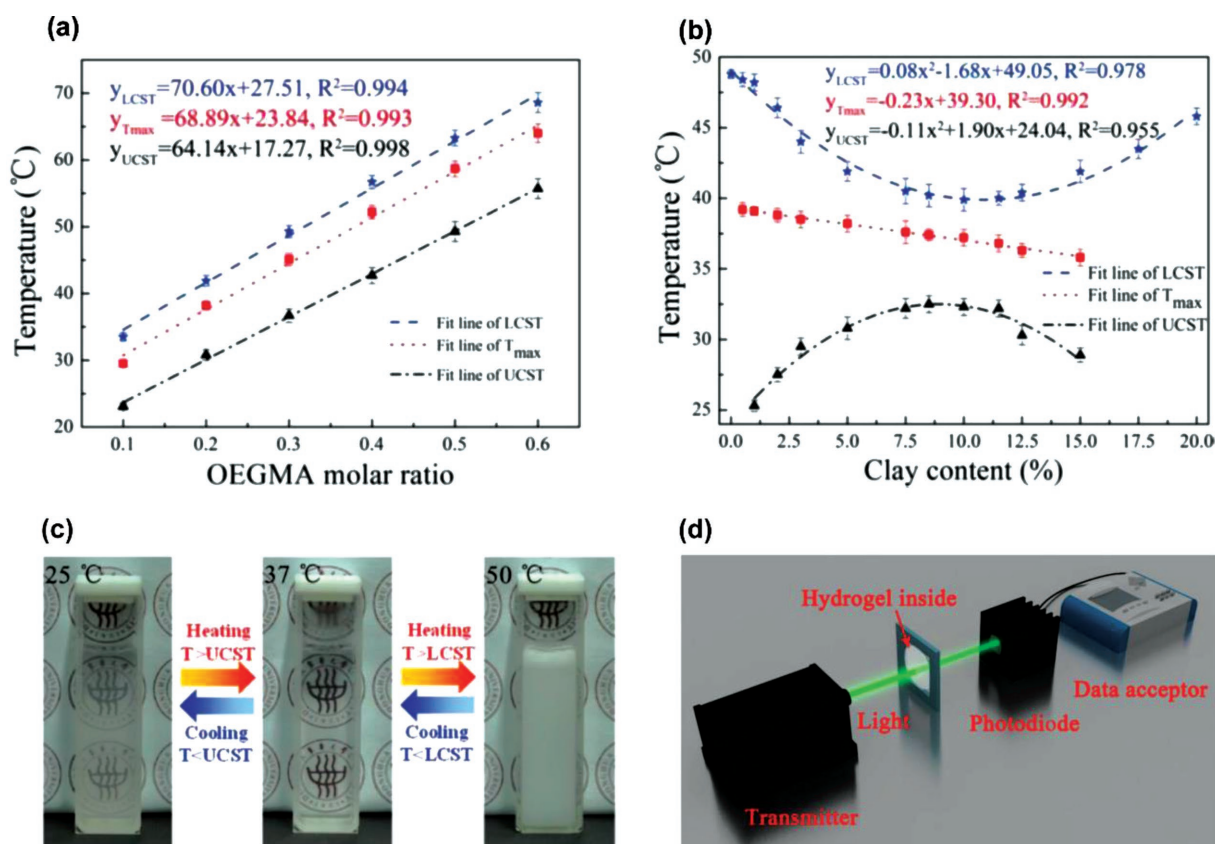


Figure 7. Temperature dependence of clay/P(MEO₂MA-*co*-OEGMA) NC gels with different a) OEGMA molar ratios and b) clay content. c) Photographs of clay NC gels at different temperatures: $25\text{ }^{\circ}\text{C}$, $37\text{ }^{\circ}\text{C}$, and $50\text{ }^{\circ}\text{C}$. d) Illustration of the NC gel as an optical transducer for detecting changes in environmental temperature. Reproduced with permission.^[4] Copyright 2015, Wiley-VCH.

it efficiently into thermal energy, which resulted in a rapid increase in local temperature and caused the volume of the hydrogel in the liquid channel to change to “valve-on.”

In addition to carbon-based materials, metal and semiconductor NPs have also been widely used to fabricate photo-thermal NC gels.^[99–101] A light-responsive P(NIPAAm-co-AAm) hydrogel incorporating silica-gold NPs as a cross-linker with photothermal conversion was reported in the use of a potential cancer therapy strategy because gold NPs can convert NIR into local heat to cause tissue necrosis and chemotherapeutic release.^[102] Recently, a novel NIR laser-switched CuS/P(MEO₂MA-co-OEGMA) NC microgel was prepared by using PVP-modified CuS as a photothermal agent.^[103] The PVP-modified CuS was dispersed homogeneously in the hydrogel, which could generate heat under remote NIR irradiation and lead to the phase transition of thermo-responsive P(MEO₂MA-co-OEGMA). This NC gel could be constructed as a smart fluidic microvalve as **Figure 8a** shows. This fast and precise response to NIR indicates the promise of NC gel for applications in intelligent drug switches.

In addition, light is ideal for the accurate remote control of the actuator. PNIPAAm/GO NC gel with asymmetrically layered structures designed to combine light-responsive properties performed a programmed shape transformation due to the inhomogeneous swelling–deswelling ratios of different layers.^[104] The photothermal conversion property of GO induced a faster temperature increase in the PNIPAAm/GO layer, which resulted in anisotropic swelling. Furthermore, gradient distribution of photothermal NPs in hydrogel matrix could lead a

gradient stress of hydrogel under NIR irradiation. For example, the external DC induced a gradient distribution of negatively charged GO in thermosensitive PNIPAAm matrix.^[75] Interestingly, these GO nanosheets were not only gradient-distributed but also formed oriented structure in the hydrogel along the direction of DC field. This NC gel with gradient and oriented structure of NPs could show unique anisotropic mechanical and light-responsive properties on macroscopic scale (Figure 8b).

3.2.4. Electro-Responsive NC Gels

Conventional electro-responsive hydrogels are usually prepared from synthetic and natural polyelectrolytes. Polyelectrolyte hydrogels are generally ion-conductive, and their electro-responsive behavior is considerably influenced by the concentration and distribution of ions.^[105] Electro-responsive hydrogels generally undergo a swelling–deswelling transition and shape variation based on changes in microstructure induced by an electric field.^[105] For example, in a drug release system, hydrogels deswelled in response to electrical stimuli for drug release, and then the charged drug moved to the electrode with the opposite charge.^[5] The electrical and mechanical properties of conventional electro-responsive hydrogels can be greatly improved by incorporating charged NPs, such as clay, CNTs, and graphene.^[106–108]

The incorporation of clays could not only enhance the mechanical properties of hydrogels but also significantly improve their organophilic properties.^[54] For example, an

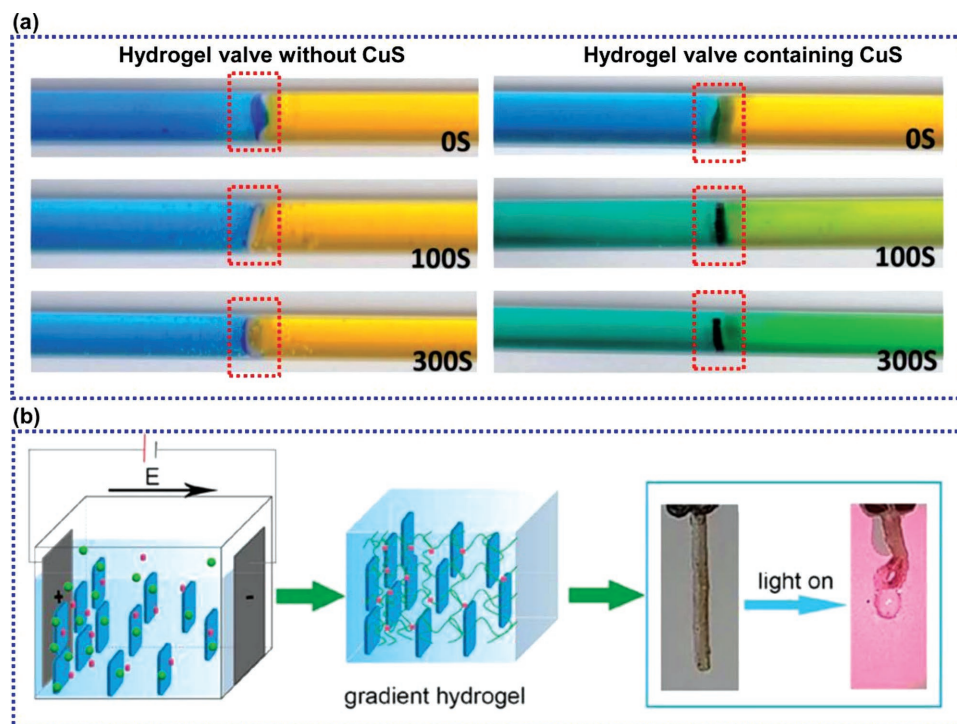


Figure 8. Light-responsive NC gel. a) Liquid hydrogel microvalves (in rectangular boxes) containing photothermal conversion NPs CuS and without CuS. The photographs show the microvalves before and after NIR irradiation. Reproduced with permission.^[103] Copyright 2017, Wiley-VCH. b) Illustration and photographs of the actuation of the PNIPAAm/GO gradient NC gel before and after irradiation. Reproduced with permission.^[75] Copyright 2018, American Chemical Society.

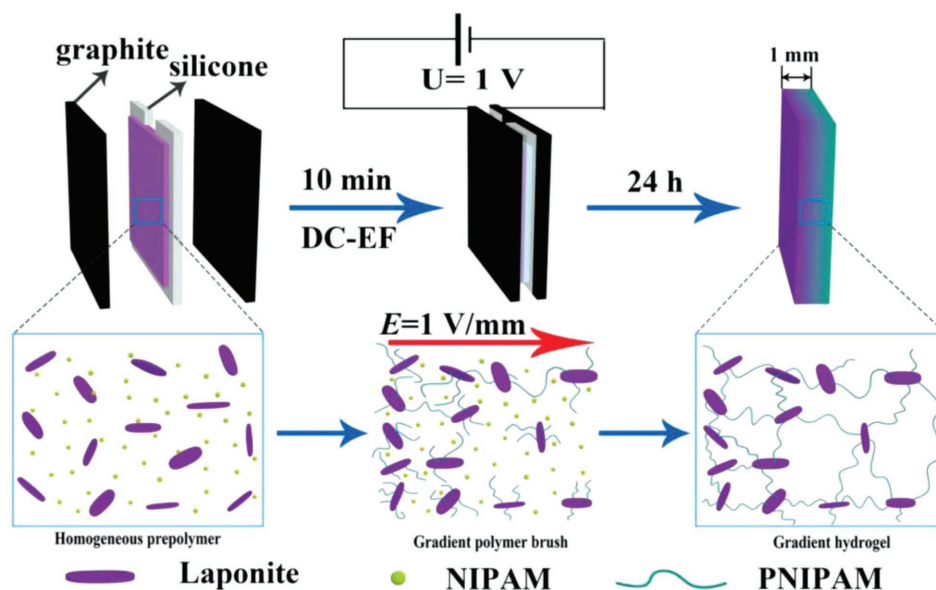


Figure 9. Schematic illustration of the preparation of the gradient PNIPAAm/clay nanocomposite hydrogel in a DC field. Reproduced with permission.^[112] Copyright 2018, Wiley-VCH.

amphiphilic chitosan–silica NC gel has been prepared in order to achieve electrically controlled drug release.^[107] The drug release was driven by the application of an electric field to the chip-like NC gel device. In this case, the electrical stimuli cause controllable drug release in vitro, ranging from burst-like to slow elution patterns due to the combination of electro-osmotic and electrophoretic mechanisms, which is convincingly related to the electrostatic interactions between hydrogel and drugs.

CNTs with excellent conductive properties could be utilized to simultaneously increase the electro-sensitivity and mechanical properties of NC gels. For example, the incorporation of multiwalled carbon nanotubes (MWCNTs) into PMAA hydrogels considerably enhanced the electro-responsiveness of hydrogels and permitted the delivery of radiolabeled sucrose in vivo over a short time under low voltage.^[109]

Reduced graphene oxide (rGO) has also been applied in electro-responsive NC gels to enable drug release. The responsiveness of PVA/rGO composite hydrogels has been investigated by using lidocaine hydrochloride as a hydrophilic substance.^[110] With the rGO content increased, the PVA/rGO hydrogel became more negatively charged, which enhanced electro-osmosis and reduced the interactions between rGO and lidocaine. Therefore, the release rate of lidocaine was increased. Compared with rGO and GO, pure graphene possesses better mechanical, thermal, and electrical properties. However, few electro-responsive NC gels have been fabricated with graphene as a nanofiller. One of the major drawbacks is the resistive heating caused by electrical stimulation. Ball-milled graphene was incorporated into an electro-responsive PMAA hydrogel, which could eliminate resistive heating due to the effective heat dissipation capabilities of PMAA hydrogels.^[111] The significant decrease in resistive heat resulting from the graphene-containing NC gels for drug release allowed a corresponding reduction in damage to skin and tissue.

In addition, electrical stimuli could induce the formation of gradient and orderly structures in NC gels. For example, a gradient structure of PNIPAAm/clay NC gels could be prepared by applying an external DC electric field during polymerization.^[73–75,112] The negative charge on the surface of the laponite tends to move toward the anode in the electric field, which induces gradient structure and anisotropic properties along the direction of the electric field (**Figure 9**).^[112] Based on the gradient structure and stimuli-responsive properties of hydrogels, a novel actuator was fabricated, which gave the gradient NC gels good prospects in the fields of tissue engineering, artificial organ, and sensor technology.

3.2.5. Magnetically Responsive NC Gels

Similar to electric fields, magnetic fields are clean and biocompatible even at clinically high field strengths. Thus, numerous examples of magnetically responsive hydrogels have been developed for various applications, including drug delivery and soft robots.^[22,96,113,114] Magnetically responsive NC gels could be prepared by the incorporation of magnetic NPs such as iron oxides ($\gamma\text{-Fe}_2\text{O}_3$, Fe_3O_4) into the hydrogel matrix. These NPs usually need to be modified with ligands or wrapped in polymer nanospheres to enable cross-linking with a hydrogel matrix.^[47] Magnetically responsive NC gels have attracted great attention in drug release systems due to their biocompatibility, fast responsiveness, and sensitivity to remote external magnetic fields. For example, Liu et al. prepared magnetically responsive NC gels by the incorporation of Fe_3O_4 NPs into PVA, which could then be applied in drug release.^[115] The dosage of the drug released could be accurately adjusted by varying the time at which the external magnetic field was applied. In the magnetic field, the Fe_3O_4 NPs became aggregated, which resulted in the decreased porosity of the PVA hydrogel. In this situation, the drug was restrained within the

compact hydrogel network, limiting the diffusion of the drug out of the hydrogel. Moreover, to avoid magnetically induced agglomeration, magnetic NPs should be stabilized by protective agents and with suitable size. For example, silica is one of the most popular protective agents. A hydrogel based on chitosan crosslinked with silylated magnetic NPs was synthesized as a drug delivery system.^[116] In this hydrogel, the magnetic NPs could be tuned from ferromagnetic to superparamagnetic by reducing their size because of the quantum size effect.^[117,118] Superparamagnetic NPs show magnetism only under an external magnetic field but become nonmagnetic without an external field, which helps to overcome agglomeration.

Metallic NPs are well known to undergo magneto-thermal conversion when magnetic fields are applied. Therefore, NC gels based on thermo-responsive hydrogels and metallic NPs could be remotely heated by external magnetic fields. For example, a biodegradable and injectable thermo-responsive NC gel based on chitosan and Fe_3O_4 has been prepared, which released the drug under a magnetic field stimulus.^[119] Similarly, alternating magnetic fields (AMFs) could also be applied to drug release from magnetically responsive NC gels. Superparamagnetic iron oxide NPs can generate heat under an AMF, which increases the temperature of the hydrogel over the phase transition temperature to result in a volume change and their emergence from the NC gel for drug diffusion.^[120]

In addition, some magnetically responsive NC gels possess self-healing properties, which contributed to the incorporation of magnetic NPs. Generally, hydrogels form fissures under stress, which can influence the integrity of the network structure, resulting in loss of functionality.^[121] However, a novel class of self-healing hydrogels possess the ability to repair them-

selves and increase the lifetime of the materials. For example, a magnetically responsive NC gel with self-healing properties was prepared by the introduction of carboxy-modified Fe_3O_4 NPs into chitosan-PEG hydrogel.^[122] The hydrogel fragments could self-heal under magnetic fields in several minutes, whereas hydrogels without magnetic NPs could not.

Furthermore, similar to the orderly structure of NC gels formed by electric fields, magnetic 2D nanosheets such as GO and titania nanosheets (TiNSs) can effectively form ordered structures within NC gels under magnetic fields.^[16,123] For example, an NC gel with a highly ordered structure was fabricated by embedding TiNSs cofacially in PNIPAAm hydrogels.^[123] Specifically, negatively charged unilamellar TiNSs aligned coaxially in a strong magnetic field, maintaining maximal electrostatic repulsion and uniform face-to-face separation (**Figure 10a**). Because of the anisotropic structures caused by electrostatically repulsive unilamellar TiNSs, the NC gels exhibited remarkable optical and mechanical anisotropies (**Figure 10b,c**).

Table 2 presents examples of NC gels that respond to temperature, light, electricity, magnetism, and pH.

4. Shaping Nanocomposite Hydrogels

Since the development of NC gels, the main fabrication approach has been a gelation-in-container process. Moreover, the tendency for thermodynamic equilibrium in gelation leads to homogeneity of the microstructure of the NC gel, which induces isotropic responses in the swelling and turbidity of the NC gel and confines its application to particular spatiotemporal

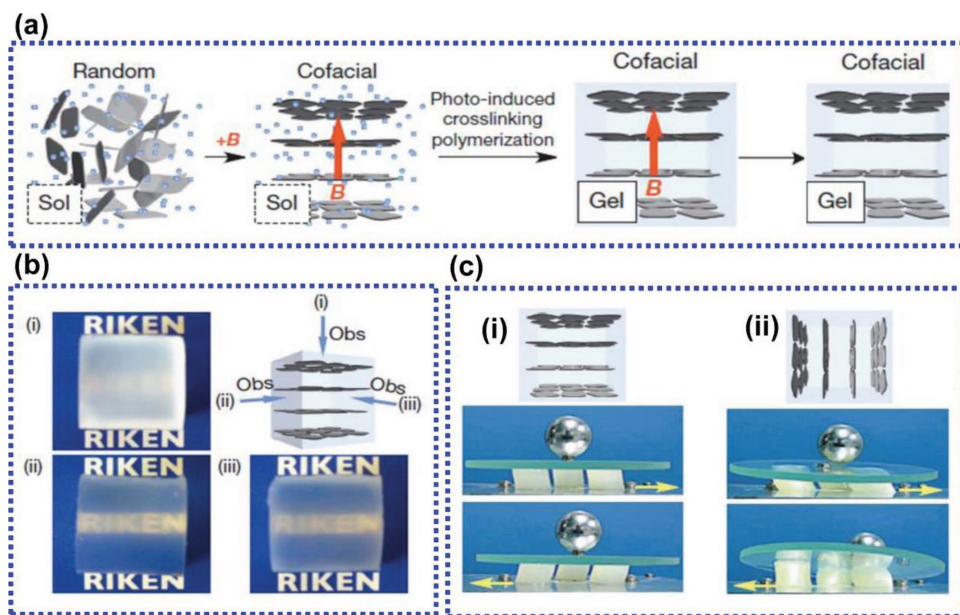


Figure 10. Cofacially oriented TiNSs/PNIPAM NC gels controlled by a magnetic field. a) Preparation of TiNSs/PNIPAM NC gels with spatial immobilization of cofacially oriented TiNSs during the gelation process under a 10 T magnetic flux. b) Optical features of the obtained NC gel viewed along directions i) orthogonal and ii,iii) parallel to the magnetically oriented TiNSs plane. c) Diagrams and photographs of demonstrations of the mechanical properties of the NC gels in vibration isolation under a mechanical oscillator: a glass stage and a metal sphere on a tee were supported by three NC gel cylindrical pillars in directions i) parallel and ii) orthogonal to the cylinder cross section. Reproduced with permission.^[16] Copyright 2015, Springer Nature.

Table 2. Examples of nanocomposite hydrogels showing different responsive properties with distinct NPs and polymers.

Nanocomposite hydrogels			
Responsive NC gels under external stimulus	NPs or polymers		Ref.
Temperature	Graphene and CNTs	PNIPAAm	[40,97]
	TiNS	PNIPAAm	[123]
	Nanoclay	P(MEO2MA-co-OEGMA)	[4,124]
Near-IR light	Graphene and GO	PNIPAAm	[98,104,125–128]
	CuS NPs	P(MEO2MA-co-OEGMA)	[103]
Electrical	CNT	PMAA	[109]
		PNIPAAm	[129]
	Graphene	PVA	[110]
		PMAA	[111]
	Silica NPs	Chitosan	[107]
	Nanoclay	PVA-g-PAA	[130]
	Magnetic	Iron oxide NPs	PVA
Chitosan			[119]
PNIPAAm			[120,131,132]
pH	Graphene	PAA	[80,94]
	CNT	P(AAm-co-SMA)	[133]
	Silver NPs	PAAm	[134]
	Nanoclay	PAA	[126]
		P(DEA-co-DMAEMA)	[135]

circumstances such as bionic devices and actuators.^[136] Currently, with the need for NC gels to act as intelligent materials to perform complex structural and functional transformations, such as biomimetic devices, robots, actuators, biomaterials, etc., numerous types of NC gel with inhomogeneous structures (gradient, orderly, hierarchical, multidimensional) have already been assembled in conjunction with specific structural and functional properties. One of the improvements in shaping NC gel is the external field-induced gelation process, which could generate a gradient and orderly microstructure in bulk NC gel. Another advance is the fabrication of NC gels with multidimensional macroscopic morphologies, such as microspheres (0D), fiber (1D), membrane (2D), and other complex macrostructure.

This section aims to provide an overview of the current advances in shaping NC gels via novel processing technology. We mainly focus on the method to produce NC gels with particular micro- or macroscale morphologies and review the specific functions of NC gels caused by inhomogeneous structures.

4.1. Bulk NC Gel with Gradient and Ordered Structures

NC gels are a promising and significant intelligent material for the formation of complex property transitions under external stimuli due to their intrinsic structural and functional properties. However, in real life, stimuli and response are always anisotropic, which means that an NC gel with homogeneous microstructure

has limitations because of the monotonous swelling and turbidity transition of the NC gel induced by homogeneity. Based on the theory above about the origin of inhomogeneities in hydrogels; however, dynamic critical fluctuations in the pre-gel solution at the onset of gelation are indispensable because these fluctuations influence the thermodynamic equilibrium of the gelation process.^[137,138] Recently, many types of external fields, such as temperature,^[139–141] mechanical strain,^[142–147] electric fields,^[148–150] and magnetic fields,^[151–153] have been introduced to generate dynamic critical fluctuations to obtain NC gels with gradient structures and other ordered structures. In Sections 3.2.4 and 3.2.5, we have overviewed the orderly distribution of NPs induced by magnetic and electrical fields. Herein, we mainly focus on the effects of other external factors, especially mechanical force and temperature, on inhomogeneity in polymer hydrogels.

Chia-Hung Chen fabricated a PPy/PNIPAAm NC gel with a well-defined gradient porous structure via the ingenious combination of thermal initiation and gradient pressure by a hydrothermal process.^[154] In this process, the free-radical vinyl polymerization and dehydration polymerization of monomers (NIPAAm and 4HBA) occurred sequentially because the novel heterobifunctional monomer (4HBA) possesses a reactive C=C bond and a less reactive –OH at either end of the molecule. The pressure gradient generated by the hydrothermal reaction resulted in a diminishing concentration gradient of the hydrogel from the top to the bottom of the hydrothermal reactor. As a result, a PPy/PNIPAAm NC gel with a gradient porous structure was obtained. This gradient structure was beneficial for performing directed shape transformation in the swelling state, which could be triggered remotely by NIR stimuli, as shown in **Figure 11**.

In addition to the gradient structure, NC gels with orderly microscopic structure have also attracted increasing attention recently due to their mechanical, optical, swelling, and other properties compared to those of homogeneous hydrogels. Two types of NC gels with orderly structures were obtained: hydrogels with oriented NP distributions and hydrogels with ordered porous structures. One strategy to achieve the orientation of NPs in the NC gel is the incorporation of nanocomposites and the application of controlled external fields. Mechanical forces, such as stretching and shearing forces, are also effective strategies to generate orderly arrangements of NPs, resulting in hydrogels with anisotropic properties. It has been reported that the distribution of clay NPs in clay/PNIPAAm NC gel was transformed from random to oriented along the stretching direction and further induced anisotropic optical properties in clay/PNIPAAm hydrogel (**Figure 12a**).^[155,156] Recently, Gong established a stretching method for the in situ synthesis of hydroxyapatite (HAp) particles with an orderly structure in a hydrogel matrix.^[142] A hydrogel containing precursors of HAp (calcium chloride and dipotassium hydrogen phosphate) was stretched to generate oriented polymer microstructures. As a result, anisotropic mineralization of HAp took place in the stretched hydrogels. The mechanism is that the elongated void-free region, which has been proven to be the region in which HAp grows, restricted the growth of HAp in the direction perpendicular to the stretching direction (**Figure 12b**). Schmidt fabricated highly extensible nanocomposite hydrogel fibers with good alignment of clay NPs, which effectively enhanced the mechanical

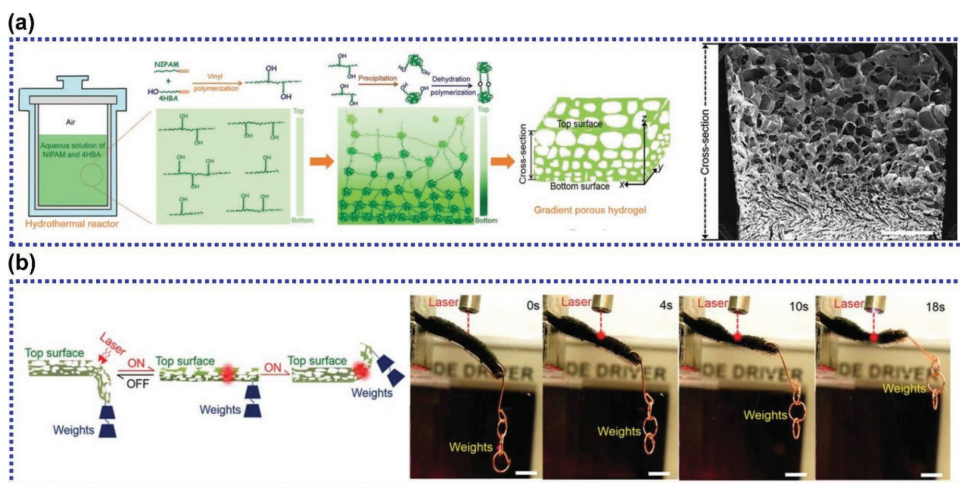


Figure 11. Hydrothermal synthesis of a gradient porous hydrogel and the process of the hydrogel lifting weights, triggered by NIR laser irradiation. a) Scheme illustrating the reaction process of the hydrothermal formation of a gradient porous hydrogel and SEM images showing a cross section view of the hydrogel. b) The process of the hydrogel lifting weights up under laser irradiation. The scale bar is 1 mm. Reproduced with permission.^[154] Copyright 2015, Wiley-VCH.

properties of hydrogels. In addition to the stretching-induced orderly distribution of hydrogel NPs, the application of shear force during the gelation process has also been shown to be a feasible strategy. Wu and Zheng reported that hydroxypropylcellulose NPs could adopt an orderly distribution in hydrogels when shear force was applied during the gelation process, resulting in anisotropic swelling and mechanical properties that do not appear in hydrogels with homogeneous structures.^[146]

In addition to the induction of orderly NP distributions by external fields, regular porous-like fibrillar, columnar, and lamellar hydrogel structures were also successfully obtained. Freeze-casting appears to be a universal strategy for the construction of NC gels with orderly porous structures because pre-gel solutions and gelled hydrogels are both suitable for freeze-casting methods. In this process, ice was used as the pore template. Due to the growth of ice crystals along the freezing direction, the polymer matrix of the hydrogel was sepa-

rated from water and formed an orderly porous structure. Ding prepared a series of NC gels with biomimetic cellular structures containing alginate and electrospun fibers by freeze-casting.^[139] These NC gels exhibited super elasticity and high water retention, and these properties were attributed to the strong orientation of the porous structural units perpendicular to the compression direction (**Figure 13**).

4.2. NC Gels with Low-Dimensional Structure

Typically, due to the fluidity of pre-gel solution, hydrogels are always fabricated in containers with a specific shape, leading to monotonous macroscopic structural properties. Recently, advances in NC gel shaping have yielded a new generation of hydrogels with diverse macroscopic structures. In addition to traditional bulk hydrogel (3D), microspheres (0D),^[47,67,157] fibers

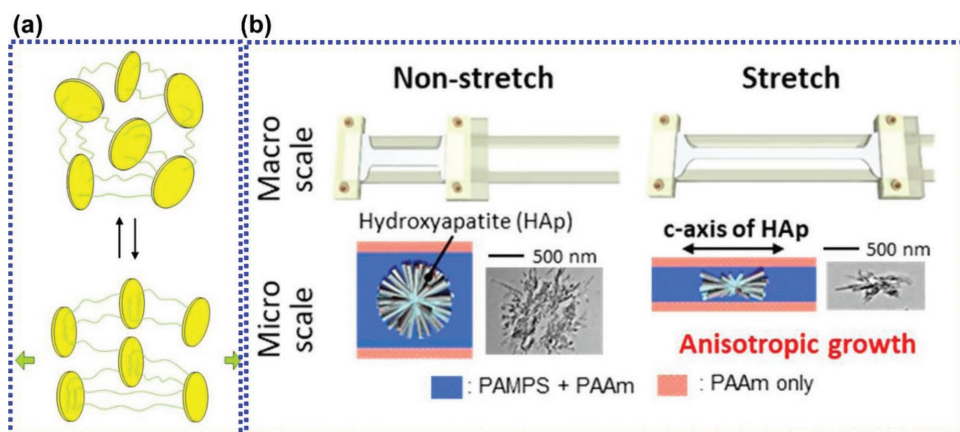


Figure 12. Hydrogels with ordered nanoparticle distribution. a) The structural changes of PNIPAAm chains and clay nanoplatelets in NC gels from random orientation to plane-orientation via uniaxial stretching. Reproduced with permission.^[156] Copyright 2014, AIP Publishing. b) Mechanism and transmission electron microscope (TEM) of the anisotropic growth of Hap crystalline rods in hydrogel. Reproduced with permission.^[142] Copyright 2017, American Chemical Society.

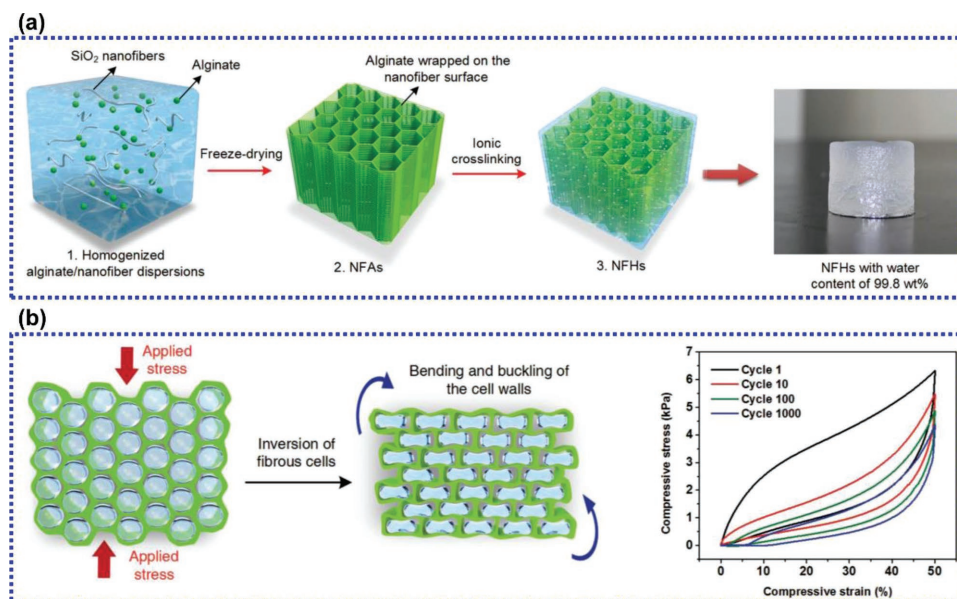


Figure 13. NC gel with ordered cellular structures obtained by freeze-casting and results of compression test. a) Schematic illustration of the freeze-casting synthesis steps: 1) homogenized alginate/nanofiber dispersions were obtained by high-speed homogenization; 2) the dispersions were freeze-dried into alginate/nanofiber composite aerogels; 3) NC gels were fabricated by Al^{3+} cross-linking; photograph of resulting NC gel. b) Schematic illustration of the inversion of the nanofibrous cell walls under compression and fatigue compression test with 1000 cycles and $\varepsilon = 50\%$. Reproduced with permission.^[139] Copyright 2017, Wiley-VCH.

(1D),^[144,158–160] membranes (2D)^[11,161] (shown in **Figure 14**), and multidimensional structures reconstructed from low-dimensional hydrogels have been shaped spatiotemporally to perform particular functions, such as in human organ replacement and soft robots. Several novel techniques, such as patterning,^[162,163] electrospinning,^[164,165] templating,^[166] microfluidics,^[167,168] and 3D printing,^[159,169,170] have been successfully established for the fabrication of NC gels with low-dimensional structures. In addition to hydrogel microspheres and membranes, which have been deeply studied for several years, hydrogel fiber is regarded as a promising low-dimensional material with particular spatiotemporal properties, such as a high length/diameter ratio, flexibility, and knittability, which are suitable for the reconstruction of complex multidimensional structures.

Extrusion,^[171] gelation in capillaries,^[78,172] and templating^[173] can produce hydrogel fibers from nanoscale to microscale with limited length. Furthermore, several novel techniques have been established to fabricate continuous hydrogel microfibers, including surface modification,^[174,175] microfluidics, electrospinning, 3D printing, and dynamic cross-linking spinning.^[176,177]

A. P. H. J. Schenning grafted a spiropyran-NIPAAm layer onto the surface of cotton fabric by ATRP.^[174] This novel hydrogel-modified textile possesses dual sensitivity to light and temperature stimuli and could be utilized in intelligent clothing for temperature and humidity management. Khademhosseini produced continuous alginate-coated PU fibers and utilized them as scaffolds in tissue engineering with diverse multiple structures by weaving technique.^[175]

A microfluidic device is a type of integrated micron-size reactor with high precision that has been widely used in nano/microgel fabrication. Recently, microfluidic spinning techniques

have been established for hydrogel fiber production because microfluidics possess a fiber-shaped channel in which fiber formation and gelation can occur simultaneously. Typically, as shown in **Figure 15a**, the microfluidic device was used to extrude nanocellulose crystal composite hydrogel fiber. Several aqueous nanoparticle suspensions (inks), which contained nanocellulose, solution of CaCl_2 , and dye with diverse color, were supplied to inlets (1)–(4) of the device. After modified with XYZ-directions, composite hydrogel fibers could be obtained in purpose.^[178] In addition, the microfluidic strategy can be used to produce fibers with diverse morphologies and multiple components, such as hollow, thermosensitive, or magneto-sensitive fibers, by the delicate design of microfluidic structures.^[167]

3D printing is an advanced technology for the fabrication of fiber-based hydrogel devices with complex macroscopic structures. In a typical 3D printing process, the pre-gel solution is extruded along a predetermined route and then gelled to form a particular fiber-based device. One of the most important parameters of 3D printing is the rheological behavior of the pre-gel solution. A pre-gel solution with excellent fluidity is not stable for 3D printing because the extruded pre-gel solution must be stable before gelation.^[179] Nanocomposite technology is an effective method to adjust the rheological behavior of the pre-gel solution. In a representative strategy, the house-of-cards structure formed by the electrostatic repulsion of clay (Laponite XLG) enhances the physical interaction between monomer and clay, thereby reducing the fluidity of the pre-gel solution. With increasing clay content, gelation occurs, but the pre-gel solution always possesses shear-thinning behavior, enabling it to undergo extrusion followed by regelation. As a result, extruded pre-gel solutions have self-supporting properties and form a fiber shape (Figure 15b).^[169] Moreover,

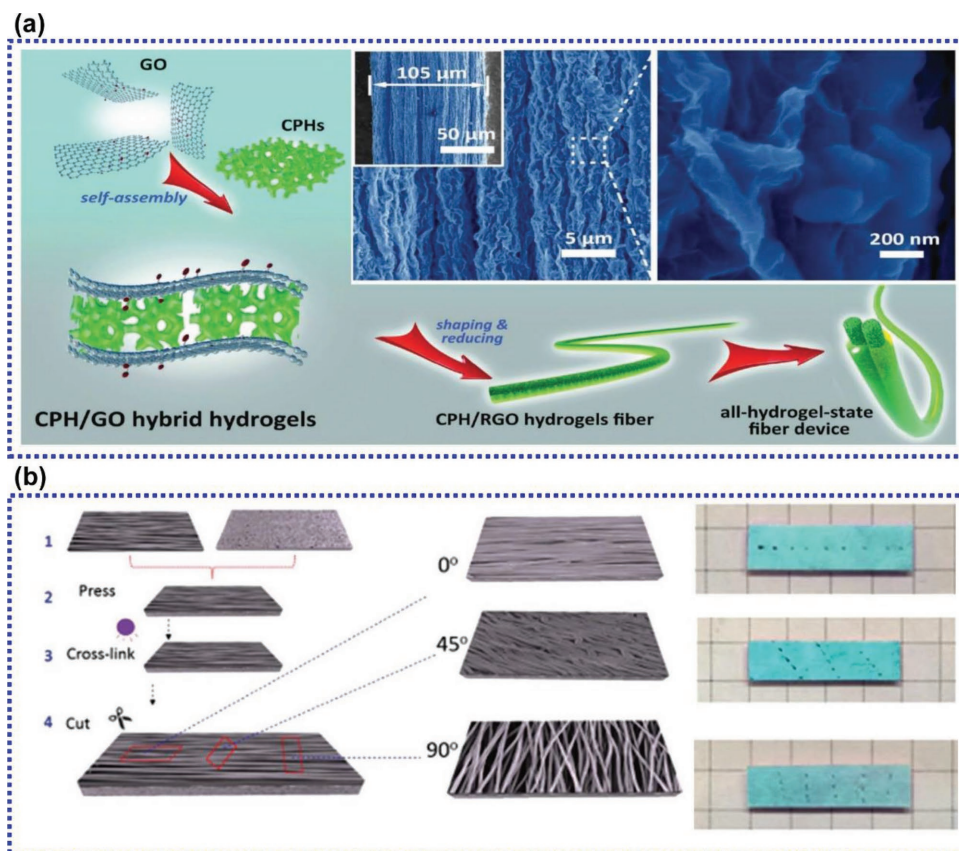


Figure 14. Low-dimensional nanocomposite hydrogels. a) Schematic illustration and morphologies images of PANI/GO composite hydrogels formation and further shaping/reduction process. Reproduced with permission.^[160] Copyright 2018, Wiley-VCH. b) Schematic and photographs of the formation of 0°, 45°, 90° bilayer PNIPAAm hydrogel by the electrospinning of aligned and random layers. Reproduced with permission.^[161] Copyright 2016, Wiley-VCH.

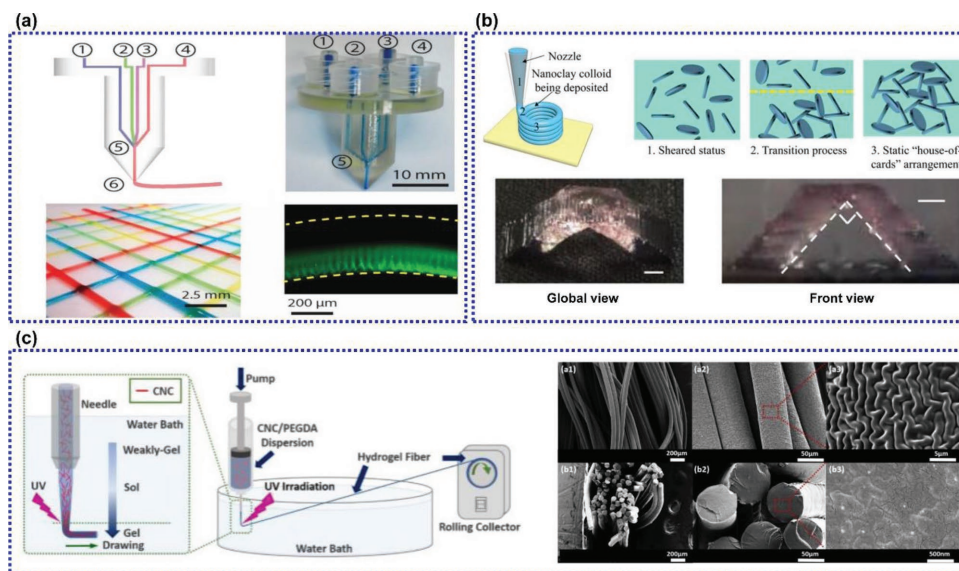


Figure 15. Three examples of hydrogel microfibers fabrication via different techniques. a) Schematic and photograph of the microfluidic device and as-prepared composite hydrogel fibers with diverse colors and fluorescence. Reproduced with permission.^[178] Copyright 2018, Wiley-VCH. b) Schematics of nanoclay-enabled 3D printing approach and photographs of printed bridge structure (scale bar: 2 mm). Reproduced with permission.^[169] Copyright 2017, American Chemical Society. c) Schematic illustration of the fabrication of CNC/PEGDA microfibers via dynamic-cross-link-spinning and the polymerization process under drawing force shown in an enlarged schematic; SEM images of the surface and cross-sectional morphology of CNC/PEGDA hydrogel microfibers in different magnifications. Reproduced with permission.^[176] Copyright 2017, Elsevier.

cellulose nanocrystals (CNC) and SiO₂ have also been utilized as rheological assistants to improve the viscoelasticity of the pre-gel solution for 3D printing.^[170,180]

Recently, we established a novel dynamic cross-linking spinning process for producing hydrogel fibers on a large scale with no complex instruments.^[176,177] The pre-gel solution was stabilized in a fiber shape by self-gravity after extrusion and then gelled by UV-induced free-radical polymerization to obtain hydrogel fiber with a precisely controlled diameter by adjusting the spinning parameters such as the extrusion rate, winding speed, and concentration. In addition, CNC/PEGDA NC fiber was successfully obtained by dynamic crosslinking spinning (DCS) during the rheological investigation of a nanocomposite pre-gel solution. The novel DCS method is convenient for the large-scale production of hydrogel fibers, which has great promises for hydrogel device reconstruction (Figure 15c).^[176]

5. Applications of Nanocomposite Hydrogels

In recent years, with the improvement of hydrogel shaping technology and functional design, NC gel-based materials have emerged as promising intelligent devices in many fields. In this section, we aim to summarize novel current applications of NC gels based on advances in their functional and structural design, including soft robots, sensors, drug delivery, and tissue engineering.

5.1. Soft Robots

Artificial soft robots are flexible devices that can perform complex and programmed motions driven by external commands. NC gels with controllable mechanical properties can convert diverse environmental stimuli, including temperature, light, humidity, phase and volume change, without structural failure, making them an ideal candidate for artificial soft robots that can perform macroscopic actuation by structure and shape transitions under external stimuli.^[11,112,113]

For use in NC gels-based soft robots, NC gels with anisotropic structures, such as asymmetric structures, gradient structures, alignment structures, etc. must be fabricated. Based on the synergistic action of each domain of NC gel with a well-designed anisotropic structure, NC gels could achieve programmed macroscopic actuation under external stimuli.^[181] An important type of hydrogel robot possesses a membrane structure. For example, a bilayer soft actuator composed of thermo-responsive CNTs/PNIPAAm NC gel and a low-density polyethylene (LDPE) substrate is shown in Figure 16a.^[182] When the actuator was placed in warm water (48 °C), the volume shrinkage of the deswelled CNTs/PNIPAAm layer generated a stretching force at the interface of the hydrogel and LDPE and then led to regional self-folding until a hydrogel cube was obtained. Moreover, the unfolding process occurred at a temperature below the LCST of PNIPAAm, which demonstrated that the shape transition process was

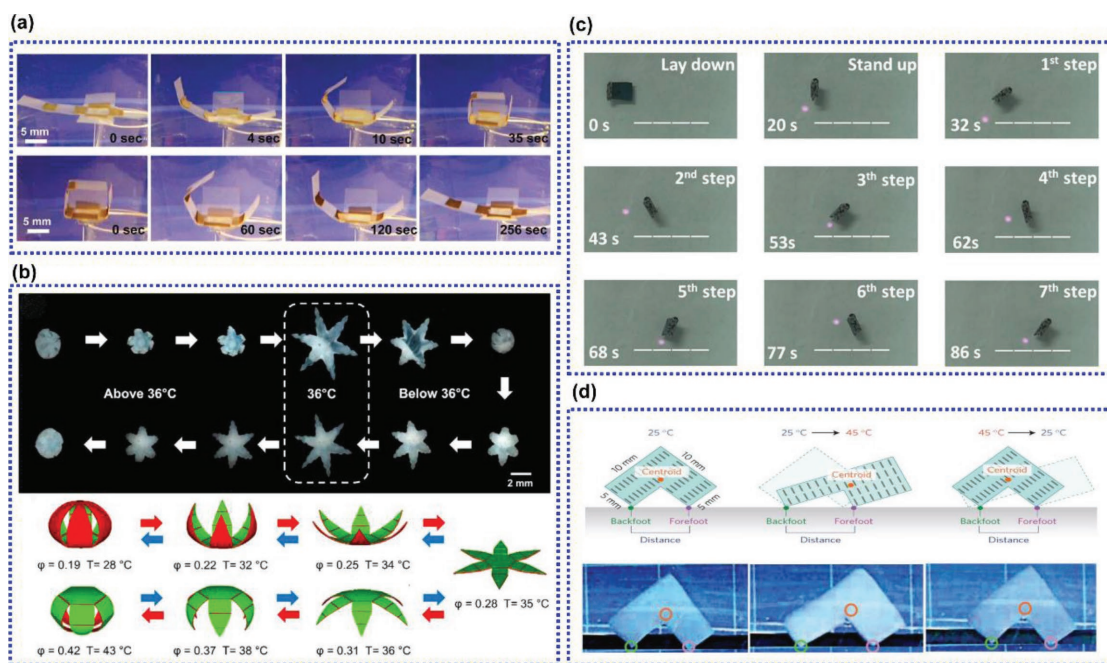


Figure 16. Soft actuator driven by responsive shape-morphing hydrogel. a) Programmable PNIPAAm cube actuators could fold in a 48 °C water bath and reversibly unfold in 20 °C. Reproduced with permission.^[182] Copyright 2011, American Chemical Society. b) Serial cycling images of a closed gripper with poly(propylene fumarate) (PPF) segments on the outside opening when the temperature was decreased to below 36 °C and then folding by itself to a closed gripper, but with the PPF segments on the inside. Simulation snapshots suggest that the extent of gripper folding depends on the temperature and the swelling function, ϕ . Reproduced with permission.^[131] Copyright 2015, American Chemical Society. c) Photographs of the light-controlled walking motion of poly(stearyl acrylate-co-methacrylic)/rGO NC gels. Reproduced with permission.^[126] Copyright 2015, Wiley-VCH. d) Unidirectional procession of microcosmically ordered structure of an NC gel actuator consisting of cofacially oriented TiNSs within a PNIPAAm hydrogel matrix. Reproduced with permission.^[123] Copyright 2015, Springer Nature.

reversible. In addition, by combining the swelling–deswelling of the NC gel layer with the non-swelled substrate layer, a soft robot that could perform bidirectional activity was obtained. For example, a set of PNIPAAm-based thermo-responsive hydrogel grippers were prepared by a serial photolithographic method.^[131] The two-layer (thermosensitive and thermo-inert layer) hydrogel grippers were actuatable and self-folding, and they exhibited bidirectional bending upon alternate heating and cooling (Figure 16b). NC gels with gradient structures also underwent programed shape transitions because of the gradient structure, which was generated by external fluctuations such as electric fields and pressures during the gelation process.

Furthermore, inspired by animals, many biomimetic robots have been fabricated based on bulk hydrogels.^[126,183] For example, the swimming bladders of fish inspired soft robots containing rGO displaying “standing” and “walking” motions under NIR laser stimuli, as shown in Figure 16c.^[126] The density of the robot was changeable via the melting/crystallizing transition of the polymer, which was induced by variations in temperature. When NIR irradiation was applied to the central part of the robot, the robot exhibited a “standing” pose. When the irradiation position was altered from left to right, the robot performed a stepwise movement. This NC gel-based robot could carry out programed movement due to the asymmetric structure generated by specified locations of the NIR stimuli.

An anisotropic hydrogel robot with an orderly structure on a microscopic scale carried out a more complicated movement.

This thermo-responsive actuator based on PNIPAAm/TiNS NC gels with an orderly structure was fabricated in a magnetic field.^[123] Due to the magnetic field–induced oriented distribution of the TiNS nanosheets, the prepared NC gels displayed an anisotropic shape transition in response to thermal stimuli (Figure 16d). After heating from 25 to 45 °C, the robot walked forward, and the centroid toward the front side was altered because of the elongation of the backfoot. In contrast, the robot moved backward after cooling down because of the backfoot shortening, but the centroid of it was restricted to a backward shift, which led to an actual forward motion. These anisotropic features of the NC gels could give rise to diverse applications that are difficult to realize with conventional hydrogels.

Currently, NC gel fiber-based materials have been developed and attracted attention because the fiber is a 1D material with an oriented structure and can be woven into a complex ordered structure. Among these materials, fiber-based biomimetic hydrogel robots have attracted much attention. Mahadevan et al. reported a series of NC gel fiber-based biomimetic plants constructed via 3D printing.^[159] These plants can transform into a complex structure after swelling because of their well-designed structures and anisotropic swelling behavior (Figure 17). This anisotropic swelling behavior occurred due to the orientation of NPs in the extrusion process and resulted in fiber that exhibited anisotropic swelling behavior and underwent a macroscopic change in shape after construction, which is beneficial for designing complex hydrogel devices to perform accurate motions.

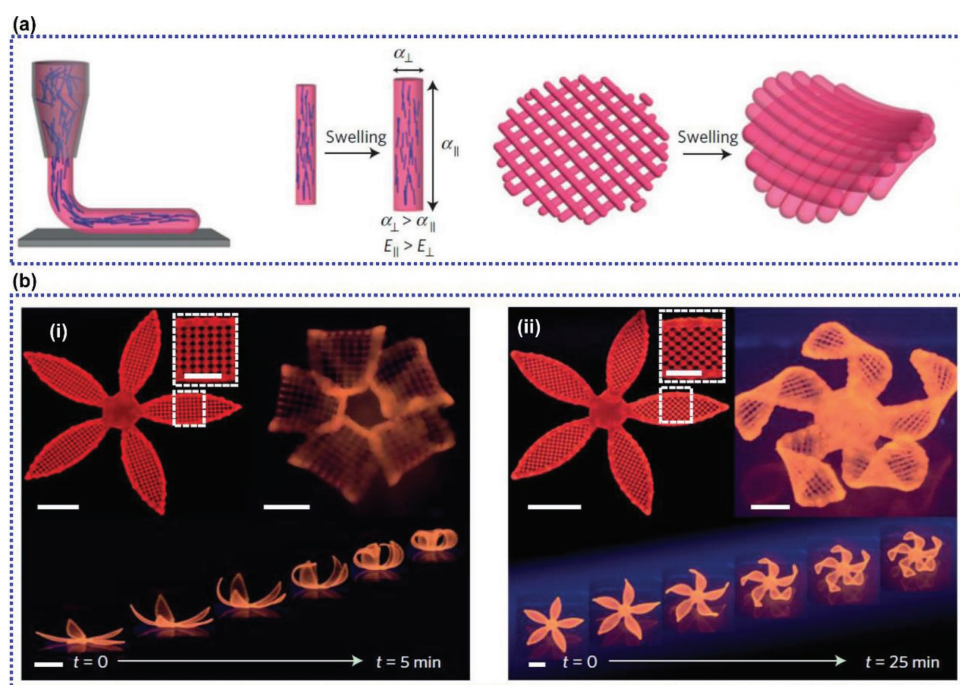


Figure 17. NC gel fiber-based biomimetic petals prepared by ink printing. a) Schematic of the shear-induced alignment of cellulose fibrils via direct ink writing, and the effects of strain (α) and stiffness (E) on anisotropic swelling behaviors of the NC gel fiber. b) The complex flower morphologies during time-lapse sequences in the swelling process with bilayers oriented at 90°/0° and 45°/45° with respect to the long axis of each petal. Reproduced with permission.^[159] Copyright 2016, Springer Nature.

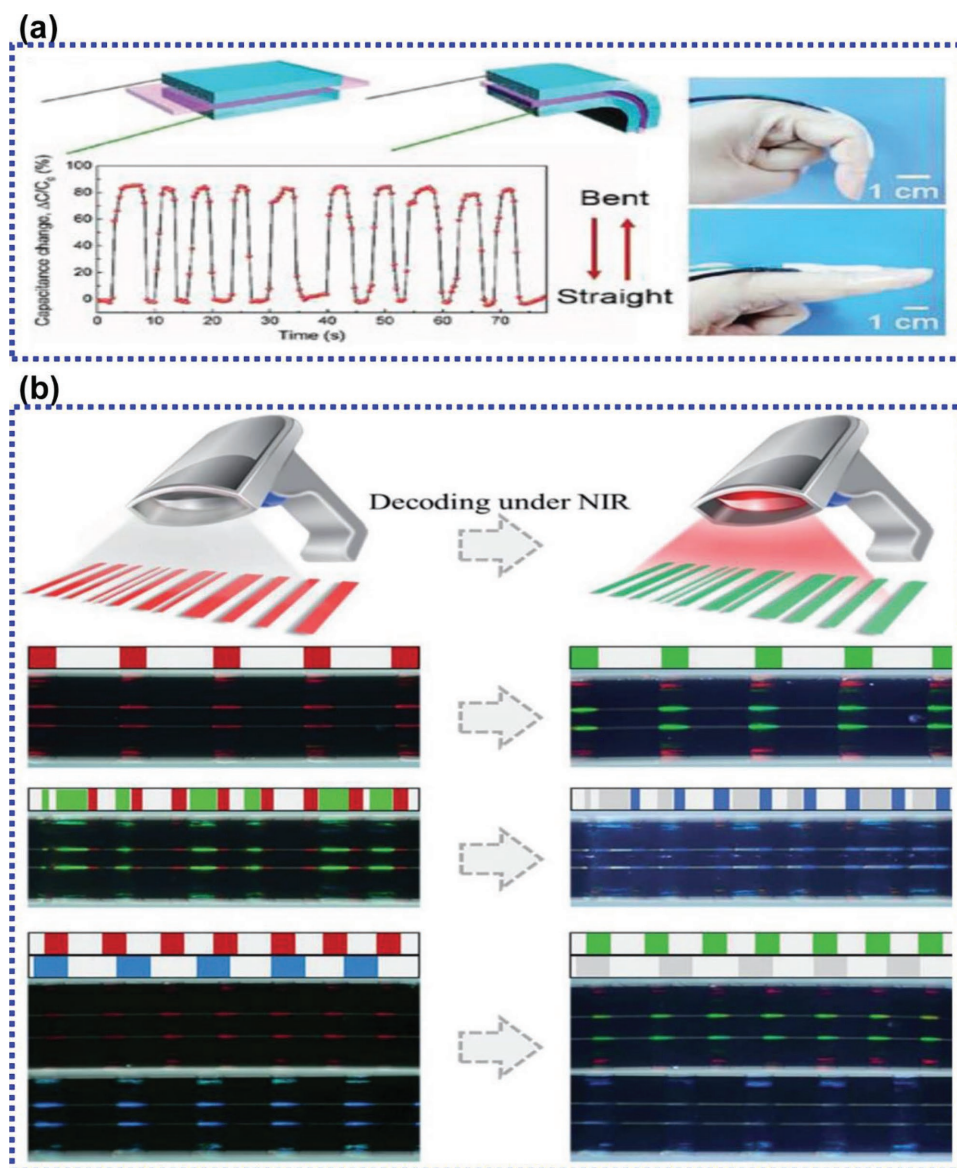


Figure 18. NC gel-based sensor and recognizer. a) Schematic design and real-time capacitance signals of PAA/amorphous calcium carbonate NC gels in the process of finger motion (bent and straight). Reproduced with permission.^[184] Copyright 2017, Wiley-VCH. b) Anti-counterfeiting property of PNIPAAm/rGO NC gel stripes as dynamic barcode labels, including monochrome stripe barcode, composite bicolor stripe barcode, and 2D stripe barcodes of structural color under NIR scanning. Reproduced with permission.^[125] Copyright 2017, Wiley-VCH.

5.2. Sensors and Recognizers

A sensor is a device that responds in a distinctive manner after receiving a signal or stimulus (strain, light, or biological elements). In contrast to actuators, strain sensors can convert mechanical energy into other types of energy, such as electrical^[184,185] and optical signals.^[186] The excellent mechanical properties and multiple stimuli-responsive properties of NC gels make them ideal materials for sensors. For example, a novel bioinspired physically cross-linked PAA/alginate/calcium carbonate NC gel was prepared as a capacitive ionic skin sensor.^[184] This NC gel-based pressure sensor was constructed by integrating two hydrogel films with a dielectric layer. According to

the relationship between deformation and capacitance, pressure-induced expansion of its area increases the capacitance of the device. This sensor can be applied to detect many types of subtle stress, including those derived from daily activities, including water droplets and human motion. As shown in **Figure 18a**, hydrogel deformation caused by finger bending led to a drastic increase in capacitance because of the conductive path variation in the hydrogel during the deformation process. The hydrogel sensor also exhibited characteristic signal patterns that could be used to detect laughter, speech, and blood pressure when attached to the throat or wrist. All these applications show the great potential of NC gels as strain sensors for use in artificial intelligence, personal healthcare, wearable devices, etc.

In addition to strain sensors, NC gels could also be applied as biosensors. For example, a semi-wet fluorescent sensor was prepared by integrating supramolecular hydrogels with MMT.^[187] Cationic coumarin dye molecules were intercalated into the space of the MMT interlayer to probe for biomarkers (spermine and spermidine) in order to evaluate the efficiency of cancer chemotherapy. The exchangeable cations of cationic fluorescent dyes aggregated on the surface of MMT and then could be replaced by polyamines through electrostatic interactions, resulting in color changes. This is a promising simple method for early cancer diagnosis.

Furthermore, an NC gel-based recognizer with NIR-responsive properties was prepared recently. rGO-based NC gels not only exhibit reversible bending behavior under NIR irradiation but can also be used as NIR-triggered dynamic barcode labels in anti-counterfeiting measures for diverse products.^[125] As shown in Figure 18b, self-assembled PNIPAAm/rGO hydrogel stripe patterns with multiple widths and colors could quickly and obviously shift from red to green in monochrome stripes, whereas a shift from red to blue and green stripes became invisible in a bicolored striped barcode. By combining two individual hydrogel stripes with different colors and compositions, 2D striped barcodes with unique hidden encoding information could be obtained.

5.3. Vehicles for Delivery and Capture

The porous structure of hydrogels permits the loading of various drugs into the polymer matrix. Moreover, the incorporation of NPs could not only avoid the undesired degradation of loaded drugs but also enable the targeted release of the drug in vivo.^[188] Cationic drugs and neutral drugs could be bound in NC gels through their interactions with negatively charged or active sites on the surfaces of NPs, such as inorganic nanoplatelets.^[189,190] For example, negatively charged MMT nanoplatelets were encapsulated in abundant doxorubicin, a neutral drug, by hydrogen bonding and electrostatic interactions within an NC gel consisting of carboxymethyl chitosan and MMT.^[191] The release of the drug from the NC gel was correlated with the breaking of the interaction and dissolution of the hydrogel. Meanwhile, the addition of MMT could improve the resistance of hydrogels to dissolution, which could affect the release rate of drugs. In addition, NC gels display responsive properties as described above, potentially enabling targeted drug release in vivo by the application of external stimuli. For example, a drug-loaded NC gel incorporating the NIR-sensitive material AuNPs into poly(*N*-acryloylglycinamide-*co*-acrylamide) (PNAAm) hydrogels could be remotely controlled by extracorporeal NIR irradiation. NIR can penetrate tissues with minimal harm, and could serve as an external stimulus to induce targeted drug release (Figure 19a).^[199]

Instead of drug delivery, NC gels could also be used as capture tools based on programmed motivation and adsorbability. For example, by applying a particular external magnetic field, a magnetic-responsive NC gel gripper could be directionally guided toward a programmed location.^[131] This type of gripper could grip and excise cells from a fibroblast cell clump at this specific location, as shown in Figure 19b. By controlling the

external magnetic field and temperature, this gripper could move to the cells that need to be excised and grip them. In addition to cell capture in vivo, the NC gel could also be used as a promising dirt cleaner in the industries.^[192,193] For example, an NC gel consisting of colloidal silica NPs and benign polysaccharides has been exploited in pipeline maintenance in a wine distillery.^[192] This type of NC gel possesses good biocompatibility, environmental degradability, and a wide processing range due to the simple chemical components of the hydrogel and its shear-thinning behavior. When pumped through the pipe, the hydrogel performed greatly and enhanced scouring of the piping over the industry standard (KOH clean method).

5.4. Tissue Engineering

Tissue engineering requires that the materials possess tissue repair and regeneration ability, which can be obtained by combining biomaterial scaffolds, biologically active factors, and stem cells.^[194] Among the various types of biomaterials, NC gel is an ideal platform in tissue engineering due to its excellent mechanical properties, high biocompatibility, and biomimetic structures.^[195,196]

Diverse types of NPs, such as hydroxyapatite (HA), CNTs, and nanoclays, have been successfully combined with biomolecules to fabricate biocompatible NC gels. Due to the specific properties of NPs and hydrogels, such NC gels have been proven as scaffolds for organizing the proliferation and differentiation of stem cells to regenerate into the desired tissue. For example, silicate nanoclays were incorporated into photo-cross-linkable gelatin hydrogels for tissue regeneration therapy.^[197] Nanoclays were shown to promote the survival, migration, proliferation, and in situ differentiation of encapsulated human stem cells due to their osteoinductive properties. The in vivo biocompatibility and local noninflammatory interactions of the implanted silicate nanoclays were investigated. The implanted NC gels were retrieved on day 3 and day 14 to examine the immune reactions of the host to the implanted hydrogels. The results illustrated that increasing the content of silicate nanoclay in the NC gel was positively related to the increase in immune cells and inflammatory cells. These experiments prove that the combination of functional NPs with biocompatible polymers is beneficial for the proliferation and differentiation of stem cells in tissue engineering and regenerative medicine.

In addition to the influence of NPs on the proliferation and differentiation of stem cells, the structural properties of hydrogels, including mechanical properties and microstructures, have been proven to influence tissue regeneration. Recently, inspired by the ordered structure of articular cartilage, a gradient hydrogel consisting of 2D nanosilicates cross-linked with cell-adhesive polymer gelatin and non-cell-adhesive polymer methacrylated kappa-carrageenan (MkCA) was prepared by a gradient of UV exposure time.^[198] The resulting gradient structure of pore size could promote cell differentiation along the scaffold for bone-cartilage regeneration. In addition, the gradient NC gels could successfully control cell encapsulation and cell morphology, which demonstrated their potential

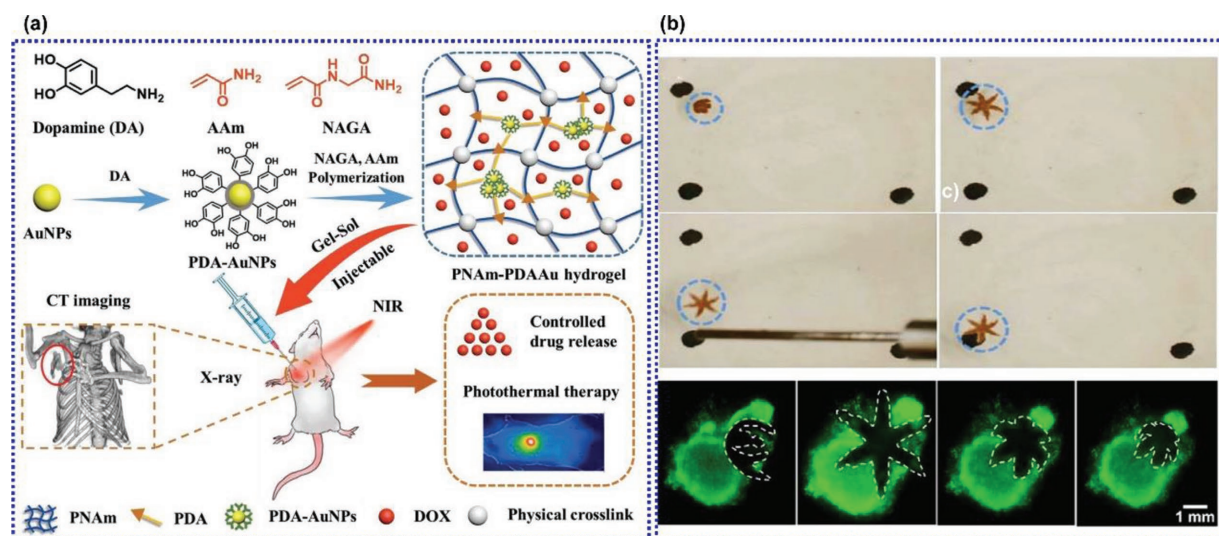


Figure 19. Nanocomposite hydrogels act as vehicle for drug delivery and cell capture. a) Schematic illustration of NIR-sensitive PNAAm/AuNPs composite hydrogel and its application of on-demand drug delivery. Reproduced with permission.^[199] Copyright 2018, Wiley-VCH. b) Poly(*N*-isopropylacrylamide-*co*-acrylic acid)/Fe₂O₃ NC gel-based thermal- and magnetic field-controlled soft grippers. (a) Grippers moved between two marks using a magnetic probe due to the magnetic sensitivity of Fe₂O₃ nanoparticles; capture and excision of cells from a live fibroblast clump; gripper with the excised cell inside. Reproduced with permission.^[131] Copyright 2015, American Chemical Society.

application to direct cell fate within the network and to direct cell differentiation without changes in the growth factors. By incorporating ordered structures and NPs, these composite hydrogel scaffolds display enhanced cell adhesion and proliferation as well as improved mechanical performance.

6. Conclusion and Outlook

From the first development in 2002 by Haraguchi, nanocomposite hydrogels have attracted increasing attention because of their specific mechanical and functional properties. In this article, we have summarized the excellent mechanical toughness and prominent responsiveness to stimuli (such as light, electricity, temperature, magnetism, and pH) of NC gels. From the perspective of structural design, recent trends have focused on incorporating inorganic NPs, such as carbon-based, metallic, nanoclay, or polymeric NPs, into 3D polymeric networks to produce NC gels with desirable functionalities for adaptation to complex environments. NC gels show great promise for applications in multiple fields, including drug delivery, smart actuators, tissue engineering, and sensors.

We hope that future publications on NC gels, from design to applications, will provide new ideas for the fabrications and applications of a new generation of functional NC gels and their devices. Although some new types of NPs with useful intrinsic properties have been introduced into NC gels, the relatively poor interfacial interactions between the polymers and NPs dramatically influenced the mechanical properties and structural stability of the hydrogels in application. Therefore, researching the surface modification of NPs remains an important approach to enhance their interfacial interaction with polymer through well-designed bonding and structure. In addition, efforts have been made to fabricate NC

gels with anisotropic structures. However, the methods for obtaining the anisotropic structure of NC gels currently rely on specific external stimuli, which are not universally practical for large-scale production. Similarly, preparing NC gels on a large scale for industrial capacity is always a challenge. Therefore, NC gels with anisotropic structures and properties need to be fabricated in large amounts. Currently, advances in processing techniques, such as 3D printing, microfluidic reactors, dynamic cross-linking spinning and extrusion, provide broad opportunities to develop large-scale NC gels with designed structures. Thus, we believe that with the continued development of processes from the design to fabrication of NC gels, new types of NC gels with orderly structures, excellent mechanical properties, and novel responses to stimuli will be fabricated for use in innovative applications in the fields of biomedicine, sensors, actuators, and biomimetic materials.

Acknowledgements

T.C. and K.H. contributed equally to this work. This work was financially supported by National Natural Science Foundation of China (No. 51733002); National Key Research and Development Program of China (2016YFA0201702/2016YFA0201700); the Fundamental Research Funds for the Central Universities (2232018A3-01); Program for Changjiang Scholars and Innovative Research Team in University (IRT 16R13); Science and Technology Commission of Shanghai Municipality (16JC1400700); Innovation Program of Shanghai Municipal Education Commission (2017-01-07-00-03-E00055); and China Postdoctoral Science Foundation (2018M631980).

Conflict of Interest

The authors declare no conflict of interest.

Keywords

mechanical properties, nanocomposite hydrogels, nanoparticle-polymer, stimuli-responsive polymers

Received: May 1, 2018
Revised: July 10, 2018
Published online:

- [1] A. K. Gaharwar, N. A. Peppas, A. Khademhosseini, *Biotechnol. Bioeng.* **2014**, *111*, 441.
- [2] Y. S. Zhang, A. Khademhosseini, *Science* **2017**, *356*, 3627.
- [3] A. Vedadghavami, F. Minooei, M. H. Mohammadi, S. Khetani, A. Rezaei Kolahchi, S. Mashayekhan, A. Sanati-Nezhad, *Acta Biomater.* **2017**, *62*, 42.
- [4] M. Xia, Y. Cheng, Z. Meng, X. Jiang, Z. Chen, P. Theato, M. Zhu, *Macromol. Rapid Commun.* **2015**, *36*, 477.
- [5] S. Merino, C. Martín, K. Kostarelos, M. Prato, E. Vázquez, *ACS Nano* **2015**, *9*, 4686.
- [6] Y. Wang, *Biomaterials* **2018**, *178*, 663.
- [7] B. Kos, *Plant Soil* **2003**, *253*, 403.
- [8] M. J. Zohuriaan-Mehr, H. Omidian, S. Doroudiani, K. Kabiri, *J. Mater. Sci.* **2010**, *45*, 5711.
- [9] K. Y. Lee, D. J. Mooney, *Chem. Rev.* **2001**, *101*, 1869.
- [10] K. Haraguchi, T. Takehisa, *Adv. Mater.* **2002**, *14*, 1120.
- [11] D. Wirthl, R. Pichler, M. Drack, G. Kettlguber, R. Moser, R. Gerstmayr, F. Hartmann, E. Bradt, R. Kaltseis, C. M. Siket, *Sci. Adv.* **2017**, *3*, 1700053.
- [12] J. P. Gong, Y. Katsuyama, T. Kurokawa, Y. Osada, *Adv. Mater.* **2003**, *15*, 1155.
- [13] Y. Okumura, K. Ito, *Adv. Mater.* **2001**, *13*, 485.
- [14] M. Zhu, Y. Liu, B. Sun, W. Zhang, X. Liu, H. Yu, Y. Zhang, D. Kuckling, H.-J. P. Adler, *Macromol. Rapid Commun.* **2006**, *27*, 1023.
- [15] K. Haraguchi, *Curr. Opin. Solid State Mater. Sci.* **2007**, *11*, 47.
- [16] M. Liu, Y. Ishida, Y. Ebina, T. Sasaki, T. Hikima, M. Takata, T. Aida, *Nature* **2015**, *517*, 68.
- [17] C. Teng, D. Xie, J. Wang, Y. Zhu, L. Jiang, *J. Mater. Chem. A* **2016**, *4*, 12884.
- [18] X. Xu, Z. Huang, Z. Huang, X. Zhang, S. He, X. Sun, Y. Shen, M. Yan, C. Zhao, *ACS Appl. Mater. Interfaces* **2017**, *9*, 20361.
- [19] A. Kumar, M. Jaiswal, *J. Appl. Polym. Sci.* **2016**, *133*, 43260.
- [20] J. Song, P. Zhang, L. Cheng, Y. Liao, B. Xu, R. Bao, W. Wang, W. Liu, *J. Mater. Chem. B* **2015**, *3*, 4231.
- [21] W. Wang, Y. Zhang, W. Liu, *Prog. Polym. Sci.* **2017**, *71*, 1.
- [22] C. Pan, L. Liu, G. Gai, *Macromol. Mater. Eng.* **2017**, *302*, 1700184.
- [23] A. A. Adewunmi, S. Ismail, A. S. Sultan, *J. Inorg. Organomet. Polym. Mater.* **2016**, *26*, 717.
- [24] A. O. Moughton, M. A. Hillmyer, T. P. Lodge, *Macromolecules* **2012**, *45*, 2.
- [25] R. T. Chacko, J. Ventura, J. Zhuang, S. Thayumanavan, *Adv. Drug Deliv. Rev.* **2012**, *64*, 836.
- [26] A. D. Schlüter, A. Halperin, M. Kröger, D. Vlassopoulos, G. Wegner, B. Zhang, *ACS Macro Lett.* **2014**, *3*, 991.
- [27] M. K. Jaiswal, J. R. Xavier, J. K. Carrow, P. Desai, D. Alge, A. K. Gaharwar, *ACS Nano* **2016**, *10*, 246.
- [28] H. Le Ferrand, S. Bolissety, A. F. Demirörs, R. Libanori, A. R. Studart, R. Mezzenga, *Nat. Commun.* **2016**, *7*, 12078.
- [29] R. Liu, S. Liang, X.-Z. Tang, D. Yan, X. Li, Z.-Z. Yu, *J. Mater. Chem.* **2012**, *22*, 14160.
- [30] C. Pan, L. Liu, Q. Chen, Q. Zhang, G. Guo, *ACS Appl. Mater. Interfaces* **2017**, *9*, 38052.
- [31] T. Zhang, T. Zuo, D. Hu, C. Chang, *ACS Appl. Mater. Interfaces* **2017**, *9*, 24230.
- [32] L. Z. Zhao, C. H. Zhou, J. Wang, D. S. Tong, W. H. Yu, H. Wang, *Soft Matter* **2015**, *11*, 9229.
- [33] X. Su, S. Mahalingam, M. Edirisinghe, B. Chen, *ACS Appl. Mater. Interfaces* **2017**, *9*, 22223.
- [34] Y. Zhao, H. Zeng, J. Nam, S. Agarwal, *Biotechnol. Bioeng.* **2009**, *102*, 624.
- [35] N. Karousis, N. Tagmatarchis, D. Tasis, *Chem. Rev.* **2010**, *110*, 5366.
- [36] C. Li, G. Shi, *Adv. Mater.* **2014**, *26*, 3992.
- [37] Q. Zhu, X. Yuan, Y. Zhu, J. Ni, X. Zhang, Z. Yang, *Nanotechnology* **2018**, *29*, 195405.
- [38] M. K. Bayazit, L. S. Clarke, K. S. Coleman, N. Clarke, *J. Am. Chem. Soc.* **2010**, *132*, 15814.
- [39] Z. Li, M. Tang, J. Dai, T. Wang, R. Bai, *Polymer* **2016**, *85*, 67.
- [40] Z. Li, M. Tang, W. Bai, R. Bai, *Langmuir* **2017**, *33*, 6092.
- [41] W. Yang, B. Shao, T. Liu, Y. Zhang, R. Huang, F. Chen, Q. Fu, *ACS Appl. Mater. Interfaces* **2018**, *10*, 8245.
- [42] A. Hajian, S. B. Lindstrom, T. Pettersson, M. M. Hamedi, L. Wagberg, *Nano Lett.* **2017**, *17*, 1439.
- [43] J. Cao, Y. Wang, C. Chen, F. Yu, J. Ma, *J. Colloid Interface Sci.* **2018**, *518*, 69.
- [44] T. Dai, C. Wang, Y. Wang, W. Xu, J. Hu, Y. Cheng, *ACS Appl. Mater. Interfaces* **2018**, *10*, 15163.
- [45] W. Wentao, F. Xiaoqiao, L. Feihu, Q. Jinjing, U. M. Muhammad, R. Wenchen, J. Benzhi, Z. Shufen, T. Bingtao, *Adv. Opt. Mater.* **2018**, *6*, 1701093.
- [46] N. Annabi, A. Tamayol, J. A. Aquillas, M. Akbari, L. E. Bertassoni, C. Cha, G. Camci-Unal, M. R. Dokmeci, N. A. Peppas, A. Khademhosseini, *Adv. Mater.* **2014**, *26*, 85.
- [47] P. Schexnailder, G. Schmidt, *Colloid Polym. Sci.* **2008**, *287*, 1.
- [48] M. Xia, Y. Wang, Y. Zhang, Y. Cheng, S. Chen, R. Wang, Z. Meng, M. Zhu, *Aust. J. Chem.* **2014**, *67*, 112.
- [49] V. Pardo-Yissar, R. Gabai, A. Shipway, T. Bourenko, I. Willner, *Adv. Mater.* **2001**, *13*, 1320.
- [50] C. T. Nguyen, R. M. Kasi, *Chem. Commun.* **2015**, *51*, 12174.
- [51] H.-Y. Mi, Z. Li, L.-S. Turng, Y. Sun, S. Gong, *Mater. Des. (1980-2015)* **2014**, *56*, 398.
- [52] U. Chatterjee, S. K. Jewrajka, S. Guha, *Polym. Compos.* **2009**, *30*, 827.
- [53] G. Marcelo, M. López-González, F. Mendicuti, M. P. Tarazona, M. Valiente, *Macromolecules* **2014**, *47*, 6028.
- [54] M. Mousa, N. D. Evans, R. O. C. Oreffo, J. I. Dawson, *Biomaterials* **2018**, *159*, 204.
- [55] J. N. Coleman, M. Lotya, A. O'Neill, S. D. Bergin, P. J. King, U. Khan, K. Young, A. Gaucher, S. De, R. J. Smith, I. V. Shvets, S. K. Arora, G. Stanton, H. Y. Kim, K. Lee, G. T. Kim, G. S. Duesberg, T. Hallam, J. J. Boland, J. J. Wang, J. F. Donegan, J. C. Grunlan, G. Moriarty, A. Shmeliov, R. J. Nicholls, J. M. Perkins, E. M. Grieveson, K. Theuwissen, D. W. McComb, P. D. Nellist, V. Nicolosi, *Science* **2011**, *331*, 568.
- [56] C.-C. Wang, L.-C. Juang, C.-K. Lee, T.-C. Hsu, J.-F. Lee, H.-P. Chao, *J. Colloid Interface Sci.* **2004**, *280*, 27.
- [57] T. R. Guimarães, T. de Camargo Chaparro, F. D'Agosto, M. Lansalot, A. M. Dos Santos, E. Bourgeat-Lami, *Polym. Chem.* **2014**, *5*, 6611.
- [58] Y. Liu, M. Zhu, X. Liu, W. Zhang, B. Sun, Y. Chen, H.-J. P. Adler, *Polymer* **2006**, *47*, 1.
- [59] S. Pedron, A. M. Pritchard, G. A. Vincil, B. Andrade, S. C. Zimmerman, B. A. C. Harley, *Biomacromolecules* **2017**, *18*, 1393.
- [60] L. W. Xia, R. Xie, X. J. Ju, W. Wang, Q. Chen, L. Y. Chu, *Nat. Commun.* **2013**, *4*, 2226.
- [61] G. L. Li, H. Mohwald, D. G. Shchukin, *Chem. Soc. Rev.* **2013**, *42*, 3628.



- [62] N. Joshi, M. Grinstaff, *Curr. Top. Med. Chem.* **2008**, *8*, 1225.
- [63] Q. Wang, J. L. Mynar, M. Yoshida, E. Lee, M. Lee, K. Okuro, K. Kinbara, T. Aida, *Nature* **2010**, *463*, 339.
- [64] Z. Shaoping, Y. L. Y. Lanry, *J. Biomed. Mater. Res. Part A* **2009**, *91A*, 114.
- [65] H. Zhang, A. Patel, A. K. Gaharwar, S. M. Mihaila, G. Iviglia, S. Mukundan, H. Bae, H. Yang, A. Khademhosseini, *Biomacromolecules* **2013**, *14*, 1299.
- [66] Y. Wu, Z. Zhou, Q. Fan, L. Chen, M. Zhu, *J. Mater. Chem.* **2009**, *19*, 7340.
- [67] Y. Wu, M. Xia, Q. Fan, M. Zhu, *Chem. Commun.* **2010**, *46*, 7790.
- [68] Z. Zhu, S. Ling, J. Yeo, S. Zhao, L. Tozzi, M. J. Buehler, F. Omenetto, C. Li, D. L. Kaplan, *Adv. Funct. Mater.* **2018**, *28*, 1704757.
- [69] Y. Zhan, H. Gao, H. Wang, Z. Xu, X. Chen, B. Liu, Y. Shi, Y. Lu, L. Wen, Y. Li, Z. Li, Y. Men, X. Feng, W. Liu, *Adv. Funct. Mater.* **2018**, *28*, 1705962.
- [70] X. Yin, Y. Zhang, Q. Guo, X. Cai, J. Xiao, Z. Ding, J. Yang, *ACS Appl. Mater. Interfaces* **2018**, *10*, 10998.
- [71] R. Xu, S. Ma, P. Lin, B. Yu, F. Zhou, W. Liu, *ACS Appl. Mater. Interfaces* **2018**, *10*, 7593.
- [72] Y. Yanagisawa, Y. Nan, K. Okuro, T. Aida, *Science* **2018**, *359*, 72.
- [73] Y. Tan, R. Wu, H. Li, W. Ren, J. Du, S. Xu, J. Wang, *J. Mater. Chem. B* **2015**, *3*, 4426.
- [74] Y. Tan, S. Xu, R. Wu, J. Du, J. Sang, J. Wang, *Appl. Clay Sci.* **2017**, *148*, 77.
- [75] Y. Yang, Y. Tan, X. Wang, W. An, S. Xu, W. Liao, Y. Wang, *ACS Appl. Mater. Interfaces* **2018**, *10*, 7688.
- [76] Y. Liu, M. Takafuji, H. Ihara, M. Zhu, M. Yang, K. Gu, W. Guo, *Soft Matter* **2012**, *8*, 3295.
- [77] S. Tasoglu, C. H. Yu, H. I. Gungordu, S. Guven, T. Vural, U. Demirci, *Nat. Commun.* **2014**, *5*, 4702.
- [78] J. Guo, X. Liu, N. Jiang, A. K. Yetisen, H. Yuk, C. Yang, A. Khademhosseini, X. Zhao, S. H. Yun, *Adv. Mater.* **2016**, *28*, 10244.
- [79] X. Tong, J. Zheng, Y. Lu, Z. Zhang, H. Cheng, *Mater. Lett.* **2007**, *61*, 1704.
- [80] J. Shen, B. Yan, T. Li, Y. Long, N. Li, M. Ye, *Soft Matter* **2012**, *8*, 1831.
- [81] W. Cui, J. Ji, Y.-F. Cai, H. Li, R. Ran, *J. Mater. Chem. A* **2015**, *3*, 17445.
- [82] M. Zhong, Y.-T. Liu, X.-M. Xie, *J. Mater. Chem. B* **2015**, *3*, 4001.
- [83] J. Liu, C. Chen, C. He, J. Zhao, X. Yang, H. Wang, *ACS Nano* **2012**, *6*, 8194.
- [84] T. Wang, S. Zheng, W. Sun, X. Liu, S. Fu, Z. Tong, *Soft Matter* **2014**, *10*, 3506.
- [85] L. Wu, M. Ohtani, S. Tamesue, Y. Ishida, T. Aida, *J. Polym. Sci. Part A Polym. Chem.* **2014**, *52*, 839.
- [86] J. Yang, S. Liu, Y. Xiao, G. Gao, Y. Sun, Q. Guo, J. Wu, J. Fu, *J. Mater. Chem. B* **2016**, *4*, 1733.
- [87] S. Liu, G. Gao, Y. Xiao, J. Fu, *J. Mater. Chem. B* **2016**, *4*, 3239.
- [88] H. Xiang, M. Xia, A. Cunningham, W. Chen, B. Sun, M. Zhu, *J. Mech. Behav. Biomed. Mater.* **2017**, *72*, 74.
- [89] C. D. Jones, J. W. Steed, *Chem. Soc. Rev.* **2016**, *45*, 6546.
- [90] F. Ullah, M. B. Othman, F. Javed, Z. Ahmad, H. M. Akil, *Mater. Sci. Eng. C Mater. Biol. Appl.* **2015**, *57*, 414.
- [91] A.-J. Xie, H.-S. Yin, H.-M. Liu, C.-Y. Zhu, Y.-J. Yang, *Carbohydr. Polym.* **2018**, *185*, 96.
- [92] L. Zang, J. Ma, D. Lv, Q. Liu, W. Jiao, P. Wang, *J. Mater. Chem. A* **2017**, *5*, 19398.
- [93] A. Alam, Y. Zhang, H.-C. Kuan, S.-H. Lee, J. Ma, *Prog. Polym. Sci.* **2017**, *77*, 1.
- [94] A. Alam, Q. Meng, G. Shi, S. Arabi, J. Ma, N. Zhao, H.-C. Kuan, *Compos. Sci. Technol.* **2016**, *127*, 119.
- [95] H. Li, R. Wu, J. Zhu, P. Guo, W. Ren, S. Xu, J. Wang, *J. Polym. Sci. Part B Polym. Phys.* **2015**, *53*, 876.
- [96] F. Zhao, D. Yao, R. Guo, L. Deng, A. Dong, J. Zhang, *Nanomaterials* **2015**, *5*, 2054.
- [97] E. Zhang, T. Wang, C. Lian, W. Sun, X. Liu, Z. Tong, *Carbon* **2013**, *62*, 117.
- [98] C.-H. Zhu, Y. Lu, J. Peng, J.-F. Chen, S.-H. Yu, *Adv. Funct. Mater.* **2012**, *22*, 4017.
- [99] C. Zhigang, W. Qian, W. Huanli, Z. Lisha, S. Guosheng, S. Linlin, H. Junqing, W. Hongzhi, L. Jianshe, Z. Meifang, Z. Dongyuan, *Adv. Mater.* **2013**, *25*, 2095.
- [100] D. Heng, D. Fengying, M. Guanghui, Z. Xin, *Adv. Mater.* **2015**, *27*, 3645.
- [101] Y. Zhou, A. W. Hauser, N. P. Bende, M. G. Kuzyk, R. C. Hayward, *Adv. Funct. Mater.* **2016**, *26*, 5447.
- [102] L. E. Strong, S. N. Dahotre, J. L. West, *J. Control. Release* **2014**, *178*, 63.
- [103] K. Hou, W. Wu, M. Xia, M. Zhu, *Macromol. Mater. Eng.* **2017**, *302*, 1700213.
- [104] E. Zhang, T. Wang, W. Hong, W. Sun, X. Liu, Z. Tong, *J. Mater. Chem. A* **2014**, *2*, 15633.
- [105] S. Murdan, *J. Control. Release* **2003**, *92*, 1.
- [106] B. Xue, M. Qin, J. Wu, D. Luo, Q. Jiang, Y. Li, Y. Cao, W. Wang, *ACS Appl. Mater. Interfaces* **2016**, *8*, 15120.
- [107] W.-C. Huang, T.-J. Lee, C.-S. Hsiao, S.-Y. Chen, D.-M. Liu, *J. Mater. Chem.* **2011**, *21*, 16077.
- [108] D. Chen, J. Yang, Y. Zhu, Y. Zhang, Y. Zhu, *Appl. Catal. B Environ.* **2018**, *233*, 202.
- [109] A. Servant, L. Methven, R. P. Williams, K. Kostarelos, *Adv. Healthc. Mater.* **2013**, *2*, 806.
- [110] H.-W. Liu, S.-H. Hu, Y.-W. Chen, S.-Y. Chen, *J. Mater. Chem.* **2012**, *22*, 17311.
- [111] A. Servant, V. Leon, D. Jasim, L. Methven, P. Limousin, E. V. Fernandez-Pacheco, M. Prato, K. Kostarelos, *Adv. Healthc. Mater.* **2014**, *3*, 1334.
- [112] Y. Tan, D. Wang, H. Xu, Y. Yang, W. An, L. Yu, Z. Xiao, S. Xu, *Macromol. Rapid Commun.* **2018**, *39*, 1700863.
- [113] J. Huang, J. Liao, T. Wang, W. Sun, Z. Tong, *Soft Matter* **2018**, *14*, 2500.
- [114] R. Fuhrer, E. K. Athanassiou, N. A. Luechinger, W. J. Stark, *Small* **2009**, *5*, 383.
- [115] T.-Y. Liu, S.-H. Hu, T.-Y. Liu, D.-M. Liu, S.-Y. Chen, *Langmuir* **2006**, *22*, 5974.
- [116] T. S. Anirudhan, D. Dilu, S. Sandeep, *J. Magn. Magn. Mater.* **2013**, *343*, 149.
- [117] T. Neuberger, B. Schöpf, H. Hofmann, M. Hofmann, B. von Rechenberg, *J. Magn. Magn. Mater.* **2005**, *293*, 483.
- [118] M. Mahmoudi, S. Sant, B. Wang, S. Laurent, T. Sen, *Adv. Drug Deliv. Rev.* **2011**, *63*, 24.
- [119] D. Zhang, P. Sun, P. Li, A. Xue, X. Zhang, H. Zhang, X. Jin, *Biomaterials* **2013**, *34*, 10258.
- [120] S. Campbell, D. Maitland, T. Hoare, *ACS Macro Lett.* **2015**, *4*, 312.
- [121] E. A. Appel, M. W. Tibbitt, M. J. Webber, B. A. Mattix, O. Veisheh, R. Langer, *Nat. Commun.* **2015**, *6*, 6295.
- [122] Y. Zhang, B. Yang, X. Zhang, L. Xu, L. Tao, S. Li, Y. Wei, *Chem. Commun.* **2012**, *48*, 9305.
- [123] Y. S. Kim, M. Liu, Y. Ishida, Y. Ebina, M. Osada, T. Sakaki, T. Hikima, M. Takata, T. Aida, *Nat. Mater.* **2015**, *14*, 1002.
- [124] M. Xia, Y. Cheng, P. Theato, M. Zhu, *Macromol. Chem. Phys.* **2015**, *216*, 2230.
- [125] Z. Zhao, H. Wang, L. Shang, Y. Yu, F. Fu, Y. Zhao, Z. Gu, *Adv. Mater.* **2017**, *29*, 1704569.
- [126] L. Wang, Y. Liu, Y. Cheng, X. Cui, H. Lian, Y. Liang, F. Chen, H. Wang, W. Guo, H. Li, M. Zhu, H. Ihara, *Adv. Sci.* **2015**, *2*, 1500084.

- [127] K. Shi, Z. Liu, Y. Y. Wei, W. Wang, X. J. Ju, R. Xie, L. Y. Chu, *ACS Appl. Mater. Interfaces* **2015**, 7, 27289.
- [128] E. Wang, M. S. Desai, S. W. Lee, *Nano Lett.* **2013**, 13, 2826.
- [129] J. Wu, Y. Ren, J. Sun, L. Feng, *ACS Appl. Mater. Interfaces* **2013**, 5, 3519.
- [130] M. Boruah, M. Mili, S. Sharma, B. Gogoi, S. K. Dolui, *Polym. Compos.* **2015**, 36, 34.
- [131] J. C. Breger, C. Yoon, R. Xiao, H. R. Kwag, M. O. Wang, J. P. Fisher, T. D. Nguyen, D. H. Gracias, *ACS Appl. Mater. Interfaces* **2015**, 7, 3398.
- [132] C. Hou, Q. Zhang, M. Zhu, Y. Li, H. Wang, *Carbon* **2011**, 49, 47.
- [133] Z. Liu, Z. Yang, Y. Luo, *Polym. Compos.* **2012**, 33, 665.
- [134] T. Endo, R. Ikeda, Y. Yanagida, T. Hatsuzawa, *Anal. Chim. Acta* **2008**, 611, 205.
- [135] L. Song, M. Zhu, Y. Chen, K. Haraguchi, *Macromol. Chem. Phys.* **2008**, 209, 1564.
- [136] T.-P. Hsu, D. S. Ma, C. Cohen, *Polymer* **1983**, 24, 1273.
- [137] F. Ikkai, M. Shibayama, *J. Polym. Sci. Part B Polym. Phys.* **2005**, 43, 617.
- [138] E. S. Matsuo, M. Orkisz, S.-T. Sun, Y. Li, T. Tanaka, *Macromolecules* **1994**, 27, 6791.
- [139] Y. Si, L. Wang, X. Wang, N. Tang, J. Yu, B. Ding, *Adv. Mater.* **2017**, 29, 1700339.
- [140] X. Zeng, L. Ye, S. Yu, R. Sun, J. Xu, C.-P. Wong, *Chem. Mater.* **2015**, 27, 5849.
- [141] M. Chau, K. J. De France, B. Kopera, V. R. Machado, S. Rosenfeldt, L. Reyes, K. J. W. Chan, S. Förster, E. D. Cranston, T. Hoare, E. Kumacheva, *Chem. Mater.* **2016**, 28, 3406.
- [142] K. Fukao, T. Nonoyama, R. Kiyama, K. Furusawa, T. Kurokawa, T. Nakajima, J. P. Gong, *ACS Nano* **2017**, 11, 12103.
- [143] Y. Wu, Z. Jiang, X. Zan, Y. Lin, Q. Wang, *Colloids Surf. B Biointerfaces* **2017**, 158, 620.
- [144] A. K. Gaharwar, P. J. Schexnailder, A. Dundigalla, J. D. White, C. R. Matos-Pérez, J. L. Cloud, S. Seifert, J. J. Wilker, G. Schmidt, *Macromol. Rapid Commun.* **2011**, 32, 50.
- [145] K. Shikinaka, Y. Koizumi, K. Kaneda, Y. Osada, H. Masunaga, K. Shigehara, *Polymer* **2013**, 54, 2489.
- [146] X. Y. Lin, Z. J. Wang, P. Pan, Z. L. Wu, Q. Zheng, *RSC Adv.* **2016**, 6, 95239.
- [147] G. K. Tummala, T. Joffe, R. Rojas, C. Persson, A. Mihranyan, *Soft Matter* **2017**, 13, 3936.
- [148] Q. Lu, S. Bai, Z. Ding, H. Guo, Z. Shao, H. Zhu, D. L. Kaplan, *Adv. Mater. Interfaces* **2016**, 3, 1500687.
- [149] D. Morales, B. Bharti, M. D. Dickey, O. D. Velev, *Small* **2016**, 12, 2283.
- [150] A. Kuijk, T. Troppenz, L. Filion, A. Imhof, R. Van Rooij, M. Dijkstra, A. Van Blaaderen, *Soft Matter* **2014**, 10, 6249.
- [151] L. Wu, M. Ohtani, M. Takata, A. Saeki, S. Seki, Y. Ishida, T. Aida, *ACS Nano* **2014**, 8, 4640.
- [152] L. Maggini, M. Liu, Y. Ishida, D. Bonifazi, *Adv. Mater.* **2013**, 25, 2462.
- [153] M. Liebi, S. Kuster, J. Kohlbrecher, T. Ishikawa, P. Fischer, P. Walde, E. J. Windhab, *ACS Appl. Mater. Interfaces* **2014**, 6, 1100.
- [154] R. Luo, J. Wu, N.-D. Dinh, C.-H. Chen, *Adv. Funct. Mater.* **2015**, 25, 7272.
- [155] K. Murata, K. Haraguchi, *J. Mater. Chem.* **2007**, 17, 3385.
- [156] J. Tang, G. Xu, Y. Sun, Y. Pei, D. Fang, *J. Appl. Phys.* **2014**, 116, 244901.
- [157] H. Ahmad, M. Nurunnabi, M. M. Rahman, K. Kumar, K. Tauer, H. Minami, M. A. Gafur, *Colloids Surf. A Physicochem. Eng. Asp.* **2014**, 459, 39.
- [158] S. Nakajima, R. Kawano, H. Onoe, *Soft Matter* **2017**, 13, 3710.
- [159] A. S. Gladman, E. A. Matsumoto, R. G. Nuzzo, L. Mahadevan, J. A. Lewis, *Nat. Mater.* **2016**, 15, 413.
- [160] P. Li, Z. Jin, L. Peng, F. Zhao, D. Xiao, Y. Jin, G. Yu, *Adv. Mater.* **2018**, 30, 1800124.
- [161] L. Liu, A. Ghaemi, S. Gekle, S. Agarwal, *Adv. Mater.* **2016**, 28, 9792.
- [162] S. J. Bryant, J. L. Cuy, K. D. Hauch, B. D. Ratner, *Biomaterials* **2007**, 28, 2978.
- [163] S. Nemir, H. N. Hayenga, J. L. West, *Biotechnol. Bioeng.* **2010**, 105, 636.
- [164] S. H. Kim, S.-H. Kim, S. Nair, E. Moore, *Macromolecules* **2005**, 38, 3719.
- [165] J. Wu, N. Wang, Y. Zhao, L. Jiang, *J. Mater. Chem. A* **2013**, 1, 7290.
- [166] X. Zhang, N. Gao, Y. He, S. Liao, S. Zhang, Y. Wang, *Small* **2016**, 12, 3788.
- [167] D. Lim, E. Lee, H. Kim, S. Park, S. Baek, J. Yoon, *Soft Matter* **2015**, 11, 1606.
- [168] M. A. Daniele, D. A. Boyd, A. A. Adams, F. S. Ligler, *Adv. Healthc. Mater.* **2015**, 4, 11.
- [169] Y. Jin, C. Liu, W. Chai, A. Compaan, Y. Huang, *ACS Appl. Mater. Interfaces* **2017**, 9, 17456.
- [170] J. Leppiniemi, P. Lahtinen, A. Paajanen, R. Mahlberg, S. Metsä-Kortelainen, T. Pinomaa, H. Pajari, I. Vikholm-Lundin, P. Pursula, V. P. Hytönen, *ACS Appl. Mater. Interfaces* **2017**, 9, 21959.
- [171] Y. Li, C. T. Poon, M. Li, T. J. Lu, B. Pingguan-Murphy, F. Xu, *Adv. Funct. Mater.* **2015**, 25, 5999.
- [172] M. Choi, M. Humar, S. Kim, S. H. Yun, *Adv. Mater.* **2015**, 27, 4081.
- [173] R. Zhang, Y. Feng, S. Ma, M. Cai, J. Yang, B. Yu, F. Zhou, *Langmuir* **2017**, 33, 2069.
- [174] J. Ter Schiphorst, M. Van Den Broek, T. De Koning, J. Murphy, A. Schenning, A. Esteves, *J. Mater. Chem. A* **2016**, 4, 8676.
- [175] M. Akbari, A. Tamayol, V. Laforte, N. Annabi, A. H. Najafabadi, A. Khademhosseini, D. Juncker, *Adv. Funct. Mater.* **2014**, 24, 4060.
- [176] K. Hou, Y. Li, Y. Liu, R. Zhang, B. S. Hsiao, M. Zhu, *Polymer* **2017**, 123, 55.
- [177] K. Hou, H. Wang, Y. Lin, S. Chen, S. Yang, Y. Cheng, B. S. Hsiao, M. Zhu, *Macromol. Rapid Commun.* **2016**, 37, 1795.
- [178] M. Alizadehgiashi, A. Gevorgian, M. Tebbe, M. Seo, E. Prince, E. Kumacheva, *Adv. Mater. Technol.* **2018**, 3, 1800068.
- [179] Y. Zhou, M. Layani, S. Wang, P. Hu, Y. Ke, S. Magdassi, Y. Long, *Adv. Funct. Mater.* **2018**, 28, 1705365.
- [180] S. Sultan, A. P. Mathew, *Nanoscale* **2018**, 10, 4421.
- [181] S. Lin, H. Yuk, T. Zhang, G. A. Parada, H. Koo, C. Yu, X. Zhao, *Adv. Mater.* **2016**, 28, 4497.
- [182] X. Zhang, C. L. Pint, M. H. Lee, B. E. Schubert, A. Jamshidi, K. Takei, H. Ko, A. Gillies, R. Bardhan, J. J. Urban, M. Wu, R. Fearing, A. Javey, *Nano Lett.* **2011**, 11, 3239.
- [183] N. Hu, L. Wang, W. Zhai, M. Sun, H. Xie, Z. Wu, Q. He, *Macromol. Chem. Phys.* **2018**, 219, 1700540.
- [184] Z. Lei, Q. Wang, S. Sun, W. Zhu, P. Wu, *Adv. Mater.* **2017**, 29, 1700321.
- [185] L. Qiu, M. B. Coskun, Y. Tang, J. Z. Liu, T. Alan, J. Ding, V. T. Truong, D. Li, *Adv. Mater.* **2016**, 28, 194.
- [186] Y. Yue, T. Kurokawa, M. A. Haque, T. Nakajima, T. Nonoyama, X. Li, I. Kajiwara, J. P. Gong, *Nat. Commun.* **2014**, 5, 4659.
- [187] M. Ikeda, T. Yoshii, T. Matsui, T. Tanida, H. Komatsu, I. Hamachi, *J. Am. Chem. Soc.* **2011**, 133, 1670.
- [188] T. Vermonden, R. Censi, W. E. Hennink, *Chem. Rev.* **2012**, 112, 2853.
- [189] J. I. Dawson, J. M. Kanczler, X. B. Yang, G. S. Attard, R. O. C. Oreffo, *Adv. Mater.* **2011**, 23, 3304.
- [190] C. J. Wu, G. Schmidt, *Macromol. Rapid Commun.* **2009**, 30, 1492.
- [191] T. S. Anirudhan, S. Sandeep, *J. Mater. Chem.* **2012**, 22, 12888.
- [192] A. C. Yu, H. Chen, D. Chan, G. Agmon, L. M. Stapleton, A. M. Sevit, M. W. Tibbitt, J. D. Acosta, T. Zhang, P. W. Franzia, R. Langer, E. A. Appel, *Proc. Natl. Acad. Sci. U. S. A.* **2016**, 113, 14255.



- [193] H. Dai, Y. Huang, H. Huang, *Carbohydr. Polym.* **2018**, *185*, 1.
- [194] N. Annabi, K. Tsang, S. M. Mithieux, M. Nikkhah, A. Ameri, A. Khademhosseini, A. S. Weiss, *Adv. Funct. Mater.* **2013**, *23*, 4950.
- [195] M. Khan, J. T. Koivisto, T. I. Hukka, M. Hokka, M. Kellomaki, *ACS Appl. Mater. Interfaces* **2018**, *10*, 11950.
- [196] M. Mehrali, A. Thakur, C. P. Pennisi, S. Talebian, A. Arpanaei, M. Nikkhah, A. Dolatshahi-Pirouz, *Adv. Mater.* **2017**, *29*, 1603612.
- [197] A. Paul, V. Manoharan, D. Krafft, A. Assmann, J. A. Uquillas, S. R. Shin, A. Hasan, M. A. Hussain, A. Memic, A. K. Gaharwar, A. Khademhosseini, *J. Mater. Chem. B* **2016**, *4*, 3544.
- [198] L. M. Cross, K. Shah, S. Palani, C. W. Peak, A. K. Gaharwar, *Nanomedicine: Nanotechnology, Biology and Medicine* **2017**, <https://doi.org/10.1016/j.nano.2017.02.022>.
- [199] Y. Wu, H. Wang, F. Gao, Z. Xu, F. Dai, W. Liu, *Adv. Funct. Mater.* **2018**, *28*, 1801000.